EUROPEAN ORGANIZATION FOR NUCLEAR RESEARCH
ORGANISATION EUROPEENNE POUR LA RECHERCHE NUCLEAIRE

CERN - PS DIVISION

PS/ BD/ Note 96-01

SOME ASPECTS OF THE TRANSVERSE BTF MEASUREMENTS OF THE COASTING BEAM IN THE CERN PS BOOSTER

A. Feschenko and L. Søby

BTF is a powerful tool to study beam characteristics and accelerator parameters. When the transverse BTF is being measured, the beam is being modulated in the transverse direction and the complex response as a function of the frequency at a fixed point of the orbit is being measured. The behaviour of the BTF is influenced by a number of parameters and characteristics: the parameters of the beam under study, the magnetic system, the impedance of the vacuum chamber as well as other factors. The peculiarity of the measurements done here is the use of the active feedback loop for measurements on special cycles during normal operation of the machine. This work is in two parts. The first part includes the analysis of the coherent processes in the beam and those effects which, according to the opinion of the authors, can really be observed. The second part is devoted to the experimental studies and to the discussion of the results of the measurements made in the CERN PS Booster. The conclusion, based on this analysis and the numerical simulations, underlines the influence of the ripple of the magnetic field. The possibility of using the restoration technique of the experimental functions is considered.

Geneva, Switzerland
2 May 1996

TABLE OF CONTENTS

INTRODUCTION

Much work has been done in which the coherent processes in the beams of circular accelerators are thoroughly investigated, both theoretically and experimentally [1-12]. One method of study of coherent processes of the parameters of the beam and the accelerator, is the method, based on measurements of a so called Beam Transfer Function (BTF). When the BTF is being measured, the beam is modulated by a force in some frequency band and the complex reaction to this excitation is measured. BTF measurements are made for both longitudinal and transverse planes. For the latter both bunched and coasting beams are examined. This present work is devoted to transverse BTF measurements of the coasting beam in the CERN PS Booster at injection (50MEV) before beginning the process of acceleration. The importance of the measurements at this period of time results from the fact that the beam losses and the final intensity strongly depend on the behavior of the beam at low energy. The qualitative analysis of the coherent processes presented, including the feedback system behavior, does not claim to be original. It reflects the understanding by the authors of the coherent processes occurring in this particular machine and in the particular measuring circuit and is used to predict the results of the real measurements.

Out of all the work done on BTF measurements there are few reliable experimental results, especially for low energy machines. As a rule the experimental results diverge strongly from the anticipated ones [13,14]. The 'distorted' results make it practically impossible to plot a stability diagram and to use all the possibilities which the BTF measurements should provide. Normally these distortions are attributed the influence of various noise sources.

Our experimental results have also been strongly perturbed. The analysis of the signals enabled an assumption to be made about the influence of instabilities of phase velocities of the coherent eigen wave modes. Further analysis of the fluctuations of currents in the bending and the quadrupole magnets as well as a simplified numerical simulation of the process, confirmed the assumption. When measuring a BTF we are dealing with an unsteady process, the typical time of measurement being larger than the typical time of variation of the characteristics of the modes, decreasing the time for a measurement requires an unacceptable degradation of the resolution in frequency. Also the time of measurement cannot be smaller than the time interval which is necessary to provide a resonant excitation of the coherent oscillations.

One of the approaches to overcome similar problems uses the technique of restoration of experimental functions, based on solving the integral Fredholm equation. The very complicated problem of taking into account the law of fluctuations of the magnetic fields can be eliminated by making beam response measurements at two frequencies simultaneously.

But a conclusion about the possibility of applying this technique cannot be made without further research and detailed simulation of the processes.

1. ANALYSIS OF THE COHERENT PROCESSES IN THE COASTING BEAM. MODES OF OSCILLATIONS.

To simplify analysis, consider the behavior of a beam in a reference frame, rotating with an angular velocity ω_0 where $\omega_0/2\pi$ is equal to the revolution frequency of the beam in the accelerator. In this reference frame the particles do not move in the azimuthal direction but execute transverse oscillations (horizontal or vertical) with the frequency $Q\omega_0$, where Q is the betatron tune or number of betatron oscillations per one revolution. For simplicity we shall consider only coherent displacements of the beam with respect to the orbit. Suppose the displacement of the beam at a fixed moment in time $t = 0$ is described by the function $y_0(\theta)$, where θ is the azimuthal coordinate varying from 0 to 2π. As all the particles execute betatron oscillations with the frequency $Q\omega_0$, the behavior of the beam both in space and time $y(\theta,t)$ can be obtained by multiplying $y_0(\theta)$ by $\sin(\omega_0 Qt+\gamma(\theta))$, where $\gamma(\theta)$ is the phase of the coherent betatron oscillation for different points θ of the orbit at a moment in time t=0.

One can write

$$y(\theta,t) = y_0(\theta)\sin[\omega_0 Qt+\gamma(\theta)] \tag{1a}$$

or

$$y(\theta,t) = [y_0(\theta)\cos(\gamma(\theta))]\sin(\omega_0 Qt)+[y_0(\theta)\sin(\gamma(\theta))]\cos(\omega_0 Qt) \tag{1b}$$

As the functions $y_0(\theta)$ and $\gamma(\theta)$ are periodic with the period 2π, then the functions $y_0(\theta)\cos(\gamma(\theta))$ and $y_0(\theta)\sin(\gamma(\theta))$ are also periodic and they can be presented as the Fourier series:

$$y_0(\theta)\cos(\gamma(\theta)) = \sum_{k=0}^{\infty}\left(d_k\cos(k\theta)+e_k\sin(k\theta)\right) \tag{2a}$$

$$y_0(\theta)\sin(\gamma(\theta)) = \sum_{j=0}^{\infty}\left(p_j\cos(j\theta)+q_j\sin(j\theta)\right) \tag{2b}$$

Substituting (2a) and (2b) into (1b) and after some not complicated but tiring trigonometric transformations one can reduce the function of the beam displacement to the following expression:

$$y(\theta,t) = a_0\sin(\omega_0 Qt+\alpha_0)+\sum_{n=1}^{\infty}\left[b_n\sin(\omega_0 Qt-n\theta+\beta_n)+c_n\sin(\omega_0 Qt+n\theta+\mu_n)\right] \tag{3}$$

One can see that the displacement of the beam in space and in time can be presented as the sum of trigonometric components. The first term in (3) represents the mode of oscillation when the phase of oscillation is the same for all the points of the orbit. This oscillation can be considered as the wave with infinite phase velocity $\pm\infty$. The rest of the components of the series (3) represent sinusoidal traveling waves, having the same frequency $Q\omega_0$, but different wave numbers n. The angular wave velocity of these waves can be written as:

$$\omega_{ph0} = \pm\frac{\omega_0 Q}{n}, \qquad n = 1,2,3..... \tag{4}$$

In the frame, rotating with the beam, the absolute values of phase velocities for a given n are equal in absolute values but differ in sign. The sign "+" corresponds to the wave, propagating in the same direction as the beam does, the sign "-" corresponds to the wave, propagating in the reverse direction. At the injection energy the values of $\frac{Q\omega_0}{n}$ for the PS Booster ($\omega_0 = 2\pi \cdot 600$ kHz, $Q_H = 4.2$ for the horizontal oscillations and $Q_V = 5.3$ for the vertical ones) are given in the table 1.

Table 1

	Horizontal plane, $Q_H = 4.2$	Fast	Slow	Fast	Slow	Vertical plane, $Q_V = 5.3$	Fast	Slow	Fast	Slow
n	$\frac{Q_H\omega_0}{n}$ $\left(10^6\frac{rad}{sec}\right)$	ω_{ph} $\left(10^6\frac{rad}{sec}\right)$	ω_{ph} $\left(10^6\frac{rad}{sec}\right)$	$\frac{\omega}{2\pi}$ (MHz)	$\left\|\frac{\omega}{2\pi}\right\|$ (MHz)	$\frac{Q_V\omega_0}{n}$ $\left(10^6\frac{rad}{sec}\right)$	ω_{ph} $\left(10^6\frac{rad}{sec}\right)$	ω_{ph} $\left(10^6\frac{rad}{sec}\right)$	$\frac{\omega}{2\pi}$ (MHz)	$\left\|\frac{\omega}{2\pi}\right\|$ (MHz)
0	$\pm\infty$	$\pm\infty$	$\pm\infty$	2.52	2.52	$\pm\infty$	$\pm\infty$	$\pm\infty$	3.18	3.18
1	2π 2.52	2π 3.12	-2π 1.92	3.12	1.92	2π 3.18	2π 3.78	-2π 2.58	3.78	2.58
2	2π 1.26	2π 1.86	-2π 0.66	3.72	1.32	2π 1.59	2π 2.19	-2π 0.99	4.38	1.98
3	2π 0.84	2π 1.44	-2π 0.24	4.32	0.72	2π 1.06	2π 1.66	-2π 0.46	4.98	1.38
4	2π 0.63	2π 1.23	-2π 0.03	4.92	0.12	2π 0.795	2π 1.395	-2π 0.195	5.58	0.78
5	2π 0.504	2π 1.104	2π 0.096	5.52	0.48	2π 0.636	2π 1.236	-2π 0.036	6.18	0.18
6	2π 0.42	2π 1.02	2π 0.18	6.12	1.08	2π 0.53	2π 1.13	2π 0.07	6.78	0.42
7	2π 0.36	2π 0.96	2π 0.24	6.72	1.68	2π 0.454	2π 1.054	2π 0.146	7.38	1.02
8	2π 0.315	2π 0.915	2π 0.285	7.32	2.28	2π 0.398	2π 0.998	2π 0.202	7.98	1.62
9	2π 0.28	2π 0.88	2π 0.32	7.92	2.88	2π 0.353	2π 0.953	2π 0.247	8.58	2.12
10	2π 0.252	2π 0.825	2π 0.348	8.52	3.48	2π 0.318	2π 0.918	2π 0.282	9.18	2.72

Suppose the frame, initially moving with the beam angular velocity ω_0, begins to slow down. Phase velocities of all the waves in this frame will change. Finally, when this frame is stopped, i.e. when transforming to the laboratory frame, phase velocities of the waves become equal to:

$$\omega_{ph} = \pm\frac{\omega_0 Q}{n} + \omega_0 \tag{5}$$

The values of ω_{ph} are also presented in the table 1. The waves with the sign "+" after transformation to the laboratory frame (eq. 5) do not change there direction of propagation or sign of the phase velocity. Phase velocities of all these waves are larger than the angular velocity of the beam ω_0, so all these waves are called fast waves. Phase velocities of the waves with the negative sign "-" are smaller than ω_0 and they are called slow waves. A fraction of these slow waves with $\left|\frac{\omega_0 Q}{n}\right| > \omega_0$ propagate in the backward direction with respect to the beam (ω_{ph} is negative). These waves are called backward waves. For example, for the horizontal oscillations, slow waves (sign "-") with $n=1,2,3$ and 4 are backward waves.

In the reference frame, rotating with the beam, a detector which can measure the frequency of the beam oscillations will register the same frequency $Q\omega_0$ for all the waves. On the contrary, in the laboratory frame the frequencies of all the waves are different. The frequency which is detected can be found as the product of the wave number and the phase velocity. Phase velocity is given by (5) and the wave number, which reflects variation of the phase in space is not changed with the frame transformation and is equal to n. Thus, the frequency of the wave, which is observed in the laboratory frame can be written as:

$$\omega = \omega_{ph} n = \omega_0 (n \pm Q) \tag{6}$$

Negative values of frequencies in (6), correspond to the backward waves. One should note, that the real measuring device will detect only absolute values of the frequencies. So, for the backward waves (6) will be written as:

$$\omega = \omega_0 (Q - n) \tag{6a}$$

The values of ω are presented in table 1. The location of the frequency lines for horizontal oscillations are shown in fig. 1.

Thus the modes of the coherent oscillations of the beam in the laboratory frame can be presented as the following traveling waves:

$$y(\theta, t) = \sin[\omega_0 (n \pm Q) t - n\theta] \tag{7}$$

for $n=1,2,3...$ and the oscillation

$$y(t) = \sin(\omega_0 Q t) \tag{8}$$

The latter can also be considered as a wave, propagating with infinite (or minus infinite) phase velocity, i.e. the expression (7) can be generalized for the case $n=0$.

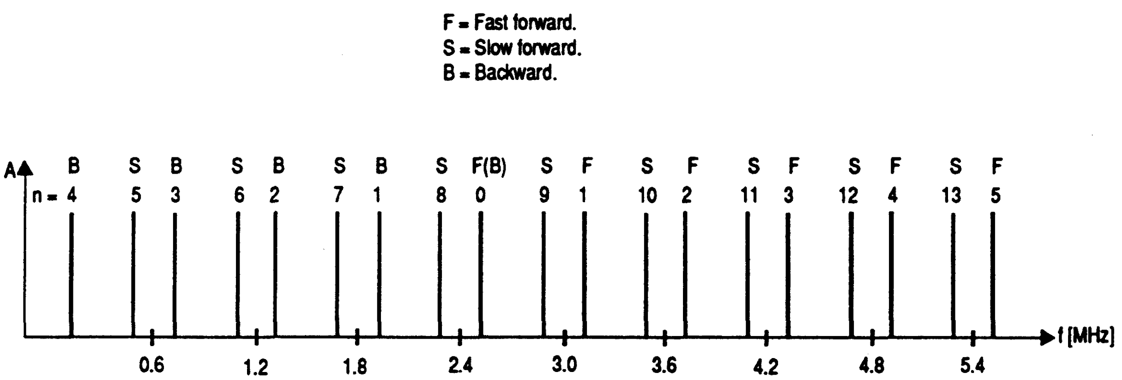

Fig. 1 : Spectra of lines for the horizontal oscillations.

2. PHYSICAL PRINCIPLES OF OPERATION OF THE TRANSVERSE FEEDBACK SYSTEM.

BTF measurements require excitation of the coherent betatron oscillations. To excite these oscillations and to measure the response of the beam the circuits of the active transverse feedback system have been used. This technique imposes some peculiarities on the process of measurement and on the interpretation of the results, so we shall qualitatively consider the operation of the feedback system, which is shown schematically in fig. 2.

Suppose there is a wave (7) of the transverse displacement of the beam. Let the detector of the beam displacement (PU) of any type be installed at the coordinate $\theta = 0$. The signal from the PU is proportional to the displacement of the beam and can be written as:

$$E_n(t) = \sin\left[\omega_0(n \pm Q)t\right]$$

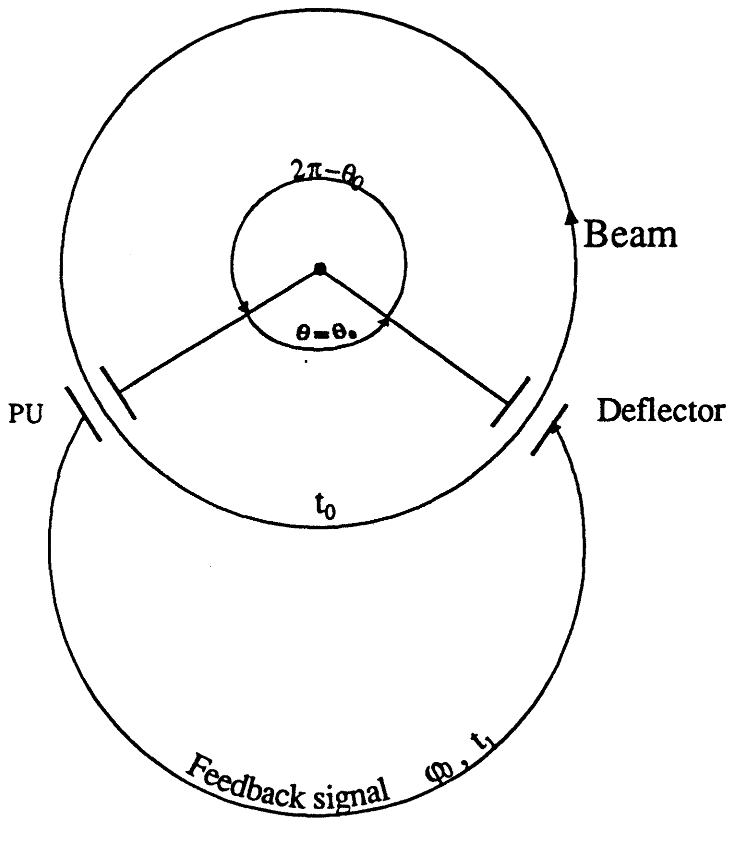

Fig. 2 : Propagation of a feedback signal

This signal propagates along the feedback line to the deflector D, installed at the coordinate $\theta = \theta_0$. Suppose the deflector is short compared with the wavelengths of the signals. In this case spatial distribution of the field of the deflector can be written as the δ-function $\delta(\theta-\theta_0)$. This space distribution can be presented as the Fourier series at the interval $[0,\ 2\pi]$:

$$E_n(\theta)=\sum_{k=0}^{\infty}a_k\cos(k\theta)+\sum_{k=0}^{\infty}b_k\sin(k\theta) \tag{9}$$

where
$$a_0=\frac{1}{2\pi}\int_0^{2\pi}f(\theta)d\theta \tag{10}$$

$$a_k=\frac{1}{\pi}\int_0^{2\pi}f(\theta)\cos(k\theta)d\theta \tag{11}$$

$$b_k=\frac{1}{\pi}\int_0^{2\pi}f(\theta)\sin(k\theta)d\theta \tag{12}$$

Substituting $f(\theta)=\delta(\theta-\theta_0)$ in (10)-(12), one can obtain:

$$a_0=\frac{1}{2\pi},\qquad a_k=\frac{\cos(k\theta_0)}{\pi},\qquad b_k=\frac{\sin(k\theta_0)}{\pi}$$

Then the spatial distribution (9) can be written as:

$$E_n(\theta)=\frac{1}{2\pi}+\frac{1}{\pi}\sum_{k=1}^{\infty}\cos(k\theta_0)\cos(k\theta)+\frac{1}{\pi}\sum_{k=1}^{\infty}\sin(k\theta_0)\sin(k\theta) \tag{13}$$

The latter expression describes the distribution of the deflecting field in space. The distribution in space and in time can de obtained by multiplying $E_n(\theta)$ by the harmonic function of time $\sin(\omega t-\varphi_0)$, where φ_0 is the phase delay of the signal in the feed back line:

$$E_n(\theta,t)=E_n(\theta)\sin(\omega t-\varphi_0) \tag{14}$$

Substituting (13) in (14), and after some transformations one can obtain:

$$E_n(\theta,t)=\frac{1}{2\pi}\sin[\omega_0(n\pm Q)t-\varphi_0]+$$
$$\frac{1}{2\pi}\sum_{k=1}^{\infty}\{\sin[\omega_0(n\pm Q)t-k\theta+k\theta_0-\varphi_0]-\sin[\omega_0(n\pm Q)t+k\theta-k\theta_0-\varphi_0]\} \tag{15}$$

The first term of (15) represents an oscillation whose phase is independent of the coordinate (a wave with infinite phase velocity). The two other terms are traveling waves, propagating in opposite directions. Thus, a single wave of the beam displacement (7) (n=const), produces an infinite number of waves of the deflecting field (k=0,1,2,3...). These waves have the same frequency $\omega=\omega_0(n\pm Q)$ but different wave numbers k and hence different phase velocities:

$$\omega_{ph} = \pm\frac{\omega_0(n \pm Q)}{k}, \qquad k = 0,1,2,3...$$

Only those waves of the deflecting field which have the same frequency and the same wave number (or the same value of phase velocity and the same direction of propagation), can interact with the wave of the beam. That is with the wave of the beam displacement (7) will interact only with that wave of deflecting field which was induced by this particular wave of the beam displacement, and which has the same wave number $k = n$. So only two terms of the series (15) can interact with the wave of the beam:

$$E(\theta,t) = \sin\left[\omega_0(n \pm Q)t - \varphi_0\right] + \sin\left[\omega_0(n \pm Q)t - n\theta + n\theta_0 - \varphi_0\right] \tag{16}$$

(In the following analysis the amplitude coefficients are taken to be equal to 1).

Consider the second term of (16):

$$E(\theta,t) = \sin\left[\omega_0(n \pm Q)t - n\theta + n\theta_0 - \varphi_0\right] \tag{17}$$

This is a traveling wave, which was originated by the beam displacement wave (7). The phases of these two waves differ by the value $n\theta - \varphi_0$. The meaning of this difference is the following: the wave of the field is delayed with respect to the wave of displacement by the value φ_0 due to delay of the signal propagation in the feedback line, simultaneously it advances the field of displacement by the phase $n\theta_0$ because it is exited at the coordinate $\theta = \theta_0$.

Our purpose is to consider the interaction of the wave of the beam displacement and the wave of the deflecting field, which is produced by this same wave of displacement via the feedback loop. When the waves are interacting, the energy is transmitted from one wave to another. As the wave of deflecting field is practically the wave of the deflecting force, it is convenient to consider its interaction not with the wave of displacement $y(\theta,t)$ but with the wave of traverse velocity $y'(\theta,t)$ of the beam. The wave of velocity is shifted in phase with respect of the wave of displacement by the value $\frac{\pi}{2}$, but the sign of this shift depends on the type of the wave (fast, slow, backward):

$$y'(\theta,t) = \sin\left[\omega_0(n \pm Q)t - n\theta \pm \frac{\pi}{2}\right] \tag{18}$$

To explain the choice of the sign one can use fig. 3. Fig. 3a shows the wave of displacement, propagating from left to right. Suppose this wave is fast, its phase velocity is greater than the velocity of the beam. Then, the velocity of the beam V_f at point A is directed with respect to the wave to the left and up. It means that the transverse velocity at this point is positive. So, the wave of velocity, shown in fig. 3b, must be attributed to the fast wave. Similarly, for the slow forward wave, the velocity V_s is directed to the right and down. The corresponding wave of velocity is shown in fig. 3c. It can be seen from these pictures, that for fast waves, the waves of velocity advance the waves of displacement by the value of $\frac{\pi}{2}$. But on the contrary, for slow forward waves the waves of velocity delay by the same value $\frac{\pi}{2}$. For backward waves the mutual direction of the wave and the particles at point A is the same as for the fast wave. So for backward waves the phase relation between the wave of velocity and the wave of displacement is the same as for the fast wave. Because the oscillation with $n=0$ can be considered as a traveling wave with infinite $\pm\infty$ phase velocity, it can be treated either as a fast or as a backward wave.

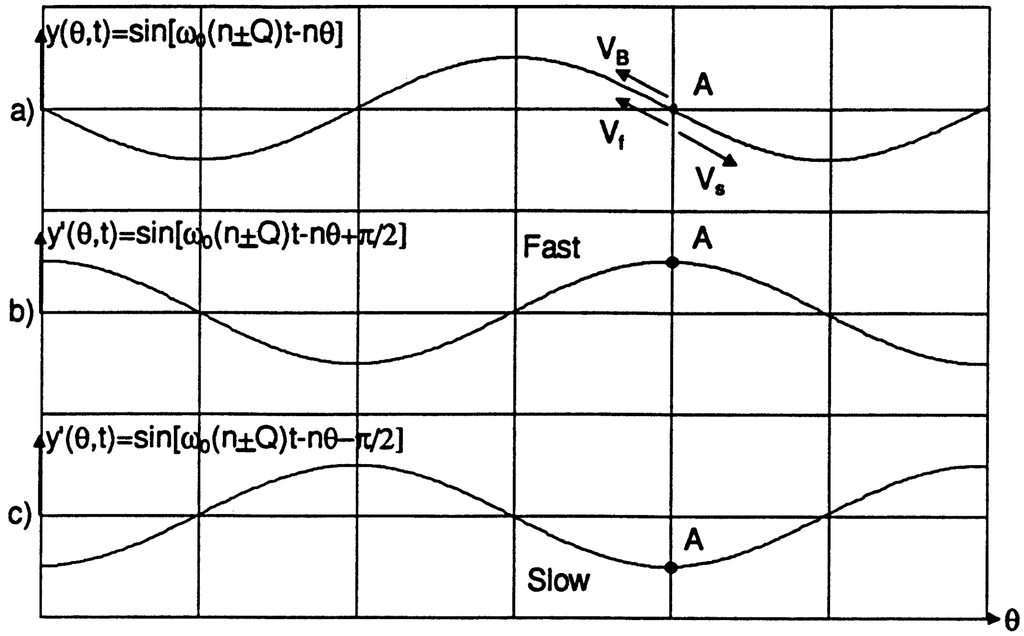

Fig. 3 : Phase shift of waves of velocity with respect to wave of displacement.

So, the "$+\frac{\pi}{2}$" in (18) corresponds to the fast and the backward waves and the "$-\frac{\pi}{2}$" to the slow forward waves.

Thus, our purpose is to consider interaction of the waves of the velocity (18) and the waves of the deflecting field (17).

Generally, their phases can differ by some constant value $\Delta\varphi$:

$$\Delta\varphi = [\omega_0(n \pm Q)t - n\theta + n\theta_0 - \varphi_0] - \left[\omega_0(n \pm Q)t - n\theta \pm \frac{\pi}{2}\right] \qquad (19)$$

which after simplification can be written as:

$$\Delta\varphi = n\theta_0 - \varphi_0 \mp \frac{\pi}{2} \qquad (20)$$

Taking into account, that

$$\theta_0 = \omega_0 t_0 \tag{21}$$

and

$$\varphi_0 = \omega_0 (n \pm Q) t_1 \tag{22}$$

where t_0 is the time of flight of the beam from the detector PU to the deflector D, t_1 is the time of propagation of the signal from PU to D along the feedback line, one can write:

$$\Delta\varphi = n\omega_0 (t_0 - t_1) \mp \omega_0 Q t_1 \mp \frac{\pi}{2} \tag{23}$$

It can be seen, that generally the value of phase difference varies for the waves with different wave numbers, and so there is a dependence of $\Delta\varphi$ on frequency. In this case it is impossible to provide the same phase difference in all the frequency bands: at some frequencies the sign of the feedback can change resulting in excitation of coherent oscillations. The necessary condition of independence of $\Delta\varphi$ on the wave number n is the equality $t_0 = t_1$. That is the times of propagation of the beam and the feedback signal from the PU to the deflector must be equal to each other. In this case:

$$\Delta\varphi = \mp\left(\frac{\pi}{2} + \omega_0 Q t_0\right) \tag{24}$$

The equality $t_0 = t_1$ means that the field acting on a particle in the deflector was induced by this particular particle in the PU. The physical meaning of the expression (24) is the following. If the phase advance $\varphi_B = \omega_0 Q t_0$ is exactly equal to $\frac{\pi}{2}$, then all the waves (fast, slow forward and backward) are in anti phase with the wave of the deflecting field ($\Delta\varphi = \pi$). If $\varphi_B = \frac{\pi}{2} + \pi$ then all these waves of the beam are in phase with the wave of the field ($\Delta\varphi = 0$). If the two latter conditions are not valid, for example if

$$\Delta\psi = \omega_0 Q t_0 - \frac{3}{2}\pi \tag{25}$$

then the waves of the beam are shifted in phase with respect to the deflecting wave by the value $\Delta\psi$. The sign of the shift (24) is the same for the fast and the backward waves and is opposite for the slow forward waves.

Another condition for proper operation of the feedback system is an optimum choice of the mutual location of PU and D (angle θ_0). Consider the integral of the interaction of the two waves, which reflects exchange of energy between the wave of the beam and the wave of the field:

$$A = \int_0^{2\pi} y'(\theta,t)E(\theta,t)d\theta \tag{26}$$

Substituting (17) and (18) in (26) for $t_0 = t_1$, one can obtain:

$$A = -\pi \sin(\varphi_B) \tag{27}$$

where $\varphi_B = \omega_0 Q t_0$ is the phase advance of the betatron oscillations from the PU to the deflector D. Fig. 4 shows the variation of the sign of the integral A for the horizontal (Q_H=4.2) and for the vertical (Q_v=5.3) planes, together with the locations of PU and the D (the electrodes of the Pu's as well as of the deflectors for the two planes are mechanically combined in the same vacuum boxes).

One should note, that for the selected positions of the PU and D the sign of the feedback can be changed for example by simply inverting the signal in the feedback line as in the CERN PS Booster Damper (fig. 5) or by interchanging the connection of the cables to the electrodes of the PU or of the D.

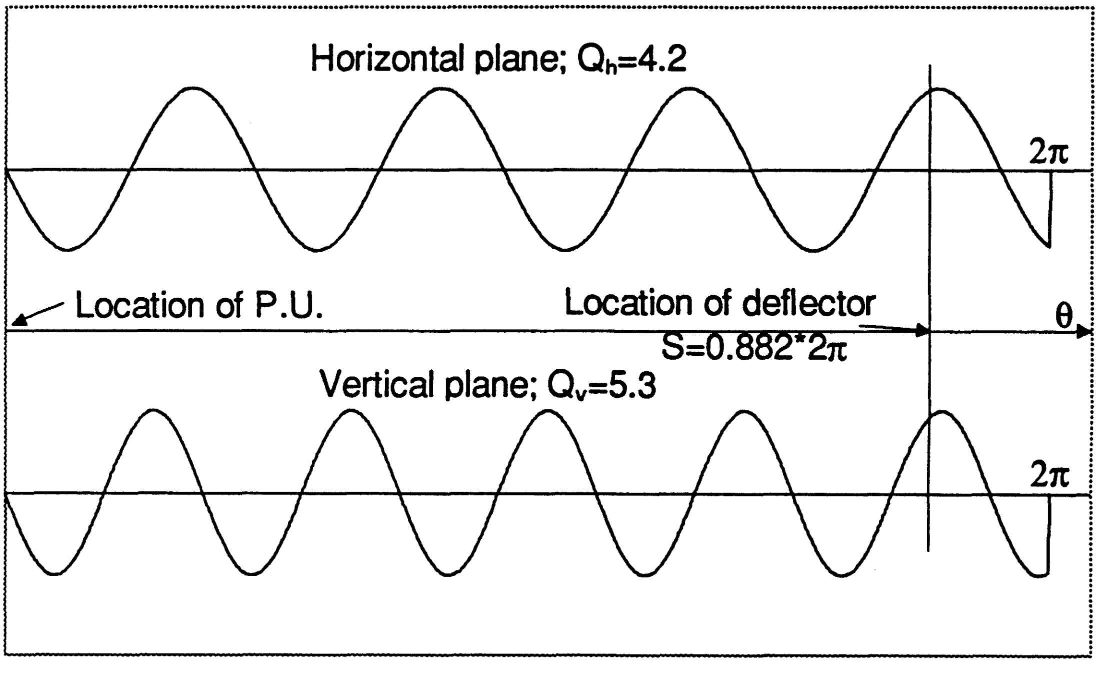

Fig. 4 : Locations of PU and Deflector of the Damper system for the horizontal and vertical planes.

3. QUALITATIVE ANALYSIS OF THE BEAM RESPONSE TO THE PERIODIC EXCITATION.

This section of the report is devoted to the qualitative analysis of the beam response, which can be observed during the BTF measurements.

As mentioned earlier, the circuits of the active feedback loop were used for the measurements. The simplified block diagram and schematic drawing of the feedback loop are shown in fig. 5 and fig. 6 respectively. To start with let us consider what will be the value of the phase difference of the signals in the real measuring circuit for the monoenergetic beam.

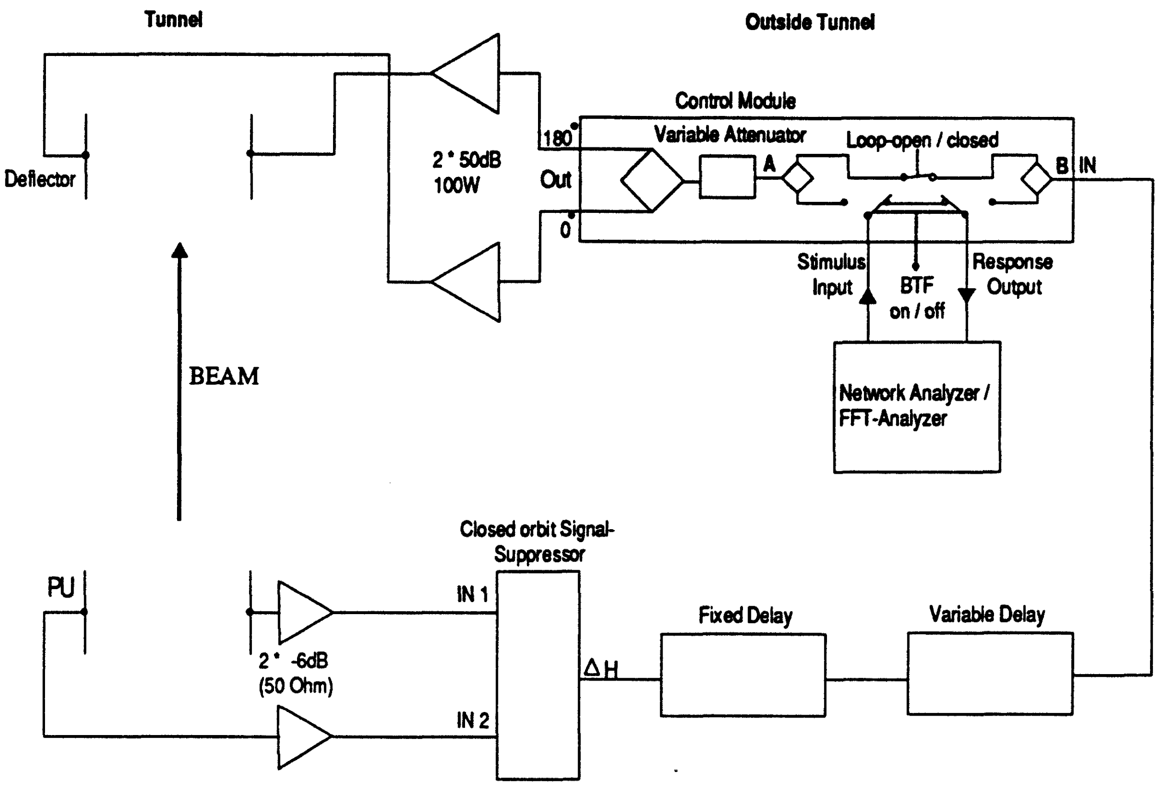

Fig. 5 : Simplified diagram of the Damper hardware.

Suppose the feedback loop is opened (the switch "Loop-open/closed" is off). The phase of the signal at point B with respect to point A can be written (see fig. 6.):

For fast and slow waves:

$$\varphi_B = \varphi_A - \varphi_1 - \varphi_2 - n(2\pi - \theta_0) \mp \frac{\pi}{2} + \pi \tag{28}$$

For backward waves:

$$\varphi_B = \varphi_A - \varphi_1 - \varphi_2 - n\theta_0 - \frac{\pi}{2} + \pi \tag{29}$$

The physical meaning of the terms in (28) and (29) is the following: φ_1-phase advance of the signal from the point A to the deflector; φ_2-phase advance of the signal from the PU to the point B; $n(2\pi - \theta_0)$-phase advance of the coherent wave of the beam

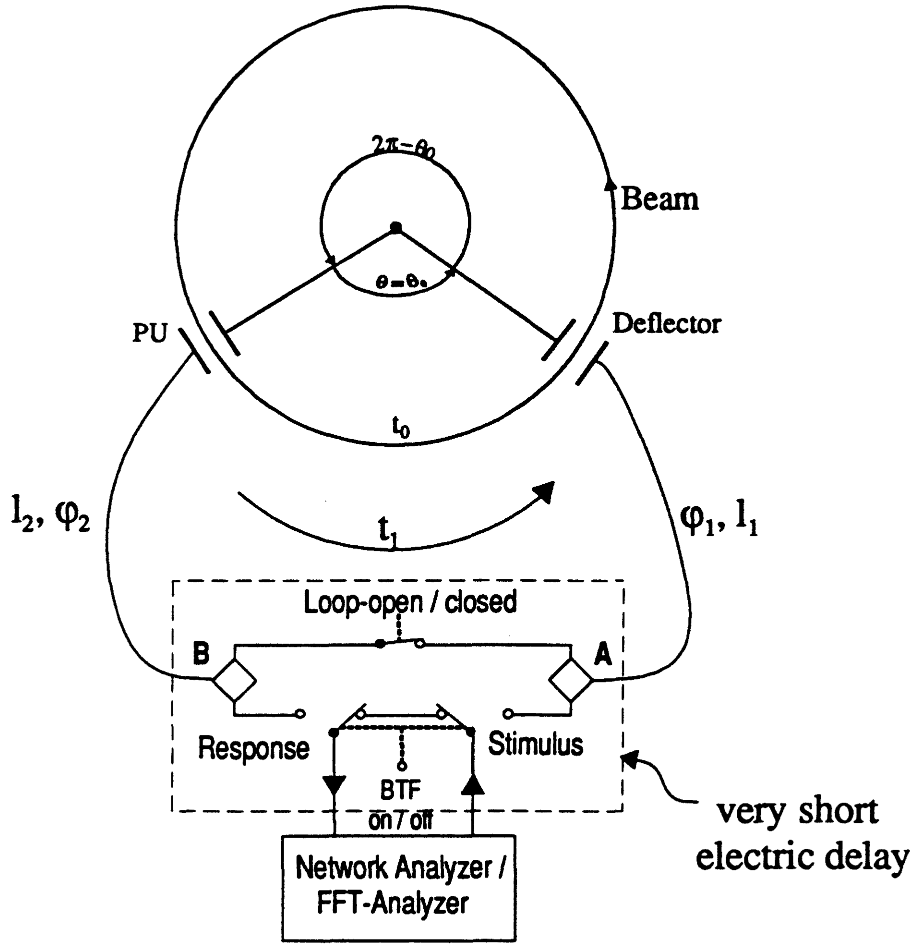

Fig. 6: Schematic drawing of the Damper system.

from the deflector to the PU for the forward waves (both the fast and the slow waves); $n\theta_0$-phase advance for the backward wave. The term $\mp\frac{\pi}{2}$ in (28) and $-\frac{\pi}{2}$ in (29) are due to the phase difference between the waves of displacement and the waves of the velocity (analogous to the (18)): the deflecting field is in phase with the wave of the velocity, while the signal which is registered by the PU is induced by the wave of displacement. The term $+\pi$ in both (28) and (29) is due to inversion of the phase in the Damper circuits (fig. 5). Substituting

$$\varphi_1 + \varphi_2 = \omega_0 (n \pm Q) t_1 \tag{30}$$

for the forward waves (fast and slow) and

$$\varphi_1 + \varphi_2 = \omega_0 (Q - n) t_1 \tag{31}$$

for the backward waves and letting $t_0 = t_1$ and $\theta_0 = \omega_0 t_0$, one can get:

$$\varphi_{AB} = \varphi_A - \varphi_B = \pm\left(\omega_0 Q t_0 - \frac{\pi}{2}\right) \tag{32}$$

Assume the phase advance of the betatron oscillations be close to the value of $\frac{3}{2}\pi$. Taking into account (25) one can represent (32) as :

$$\varphi_{AB} = \pi \pm \Delta\psi \tag{33}$$

The sign "+" here relates to the fast and backward waves and "-" to the slow ones.

Up to now we supposed that the beam is monoenergetic. Real beams have an energy spread. The difference within the pulse of particles from the nominal value $\frac{\Delta p}{p}$ results in the difference of the revolution frequency

$$\frac{\Delta\omega_0}{\omega_0} = \eta\frac{\Delta p}{p} \tag{34}$$

and of the betatron tune

$$\frac{\Delta Q}{Q} = \zeta\frac{\Delta p}{p} \tag{35}$$

Here $\eta = \frac{1}{\gamma^2} - \frac{1}{\gamma_{tr}^2}$, γ_{tr}-transition energy, normalized by the rest energy, ζ-chromaticity. Differentiating (6) and (6a) and substituting (34) and (35), one can find how the frequency of the detected signals varies when the energy of the beam changes:

For the fast waves:

$$\Delta\omega = \omega_0\frac{\Delta p}{p}\left[\eta(n+Q) + \zeta Q\right] \tag{36}$$

For the slow waves:

$$\Delta\omega = \omega_0\frac{\Delta p}{p}\left[\eta(n-Q) - \zeta Q\right] \tag{37}$$

For the backward waves

$$\Delta\omega = \omega_0\frac{\Delta p}{p}\left[\eta(Q-n) + \zeta Q\right] \tag{38}$$

If the distribution in frequency has been measured, then the energy distribution in the beam can be found using (36)-(38) by simple linear scaling. Sometimes it is convenient to present $\Delta\omega$ as a function of the frequency observed experimentally.

Fig. 7 shows the dependence of the normalized parameter $\frac{\Delta\omega}{\omega_0} \Big/ \frac{\Delta p}{p}$, found from (36)-(37) for the horizontal oscillations (ζ =-0.89 and η =0.844 [15]), on the frequency which can be detected experimentally.

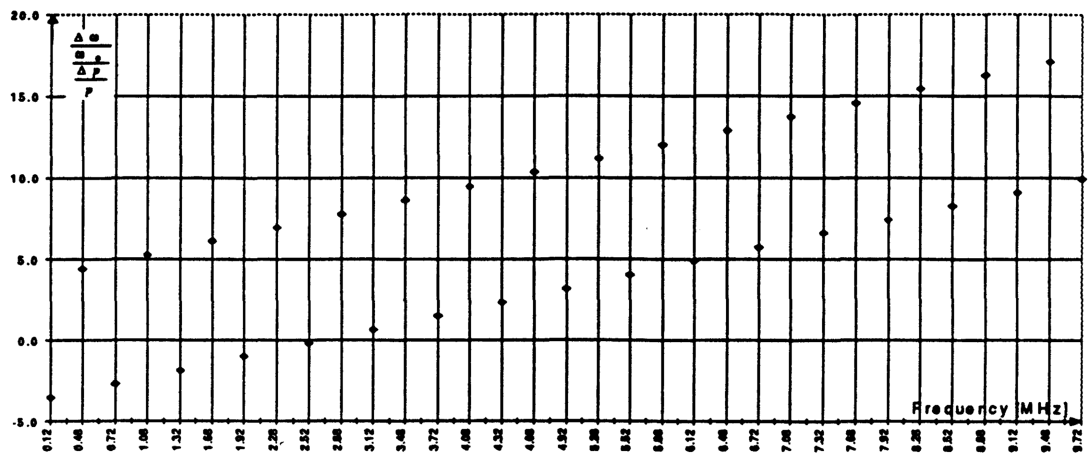

Fig. 7 : Relation between frequency spread and energy spread.

The distribution in frequencies can be found from the experimental results of the BTF measurements. We shall not reproduce here the rigorous physical and mathematical analysis of the problem which has become classical, but consider it qualitatively.

Suppose we have an array of loss less independent oscillators with slightly different frequencies. Fig. 8 [7] shows the frequency responses of the individual oscillators and the average response of a large number of oscillators. The average response depends on the distribution of the oscillators resonant frequencies. It is shown [1] that the complex function of the average response of a large number of loss less independent oscillators, with the distribution function of resonant frequencies $G(\Omega)$, normalized by the amplitude of the exiting force F_m can be written as:

$$\frac{\overline{Y}}{F_m} = -K\left[PV\int_{-\infty}^{+\infty}\frac{G(\Omega)}{\omega-\Omega}d\Omega + \pi j G(\Omega)\right] \quad (39)$$

where

$$PV\int_{-\infty}^{+\infty}\frac{G(\Omega)}{\omega-\Omega}d\Omega = \lim_{\varepsilon\to 0}\left[\int_{-\infty}^{\omega-\varepsilon}\frac{G(\Omega)}{\omega-\Omega}d\Omega + \int_{\omega+\varepsilon}^{+\infty}\frac{G(\Omega)}{\omega-\Omega}d\Omega\right] \quad (40)$$

is the real Cauchy's principal value of the integral, and K is a positive constant coefficient for a given system of oscillators.

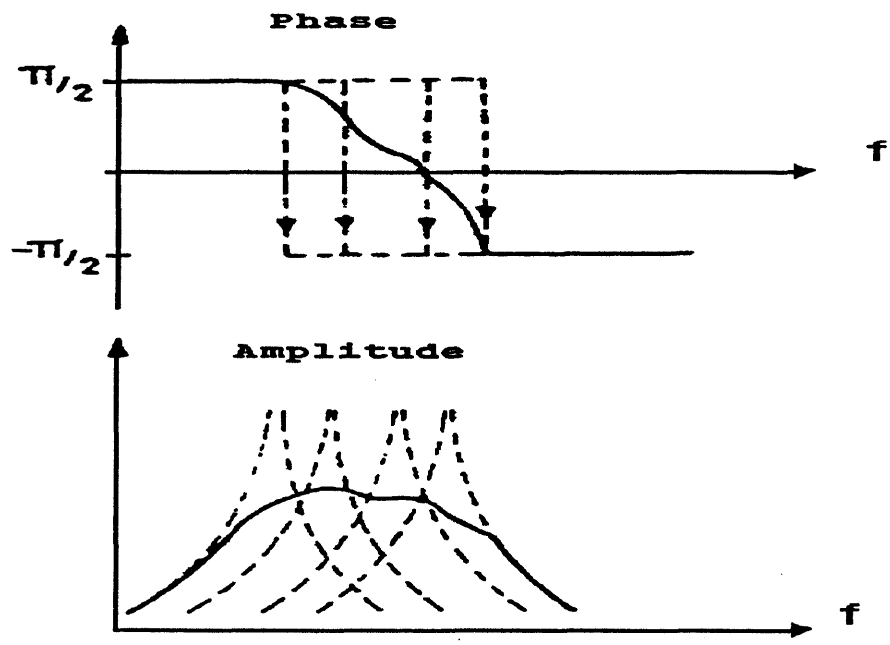

Fig. 8 : Response of oscillators to excitation and the average response (Solid line).

Similarly, one can obtain the coherent response of the beam. For the simplest case, when both the detector and the deflector are located at the same coordinate $(\theta_0 = 0)$, the response appears to be the same as for the system of oscillators except for changing the sign for the slow waves:

$$\frac{\bar{Y}}{F_m} = \mp K\left[PV + \pi j G(\Omega)\right] \tag{41}$$

The signs in (41) can be qualitatively understood from the following considerations. Similarly to lossless independent oscillators, for fast and backward waves the displacement is delayed with respect to the velocity (fig. 3) which is associated with the wave of the exiting force by $\frac{\pi}{2}$. So the sign "-" in (41) is attributed to the fast and the backward waves similarly to the case of lossless independent oscillators (39). On the contrary for slow waves, the wave of displacement advances the wave of displacement by the same value $\frac{\pi}{2}$. So the waves of displacement for slow waves are displaced with respect to the waves of displacement for the fast waves by half a period, thus providing the different signs in (41).

Sometimes it is more convenient to analyze not the function $\bar{Y}/F_m$, but the inverse function F_m/Y, which can be written as:

$$\frac{F_m}{Y} = \mp K_1[PV - \pi jG(\Omega)] \tag{42}$$

Now continue the qualitative analysis of the data, which can be obtained experimentally.

As mentioned above the phase difference of the signals between the points A and B (fig. 6)can be found from (31) or from (33), if the phase advance of the betatron oscillations between the PU and deflector is close $\frac{3}{2}\pi$. The behavior of the signal at the point B near the resonance can be written as:

$$y = A(\omega)e^{j[\varphi(\omega)\pm\Delta\psi+\pi]} \tag{43}$$

Here $A(\omega)$ and $\varphi(\omega)$ are the amplitude and the phase responses. When passing through the resonance the phase response function changes from $+\frac{\pi}{2}$ to $-\frac{\pi}{2}$. The qualitative behavior of the functions $\varphi(\omega)\pm\Delta\psi+\pi$ and $A(\omega)$ is shown in fig. 9a (here we have according to (25) and fig. 4 supposed $\Delta\psi<0$).

Consider the inverse function

$$\frac{1}{y} = \frac{1}{A(\omega)}e^{j[-\varphi(\omega)\mp\Delta\psi-\pi]} \tag{44}$$

Qualitative behavior of the amplitude $1/A(\omega)$ and the phase $-\varphi(\omega)\mp\Delta\psi-\pi$ characteristics is shown in fig. 9b.

It is convenient to draw the function $1/y$ in the complex plane (fig. 10). Each point of the curve (for example point A) is characterized by the vector with the modulus $1/A(\omega)$ rotated with respect to the positive direction of the real axis by the angle $-\varphi(\omega)\mp\Delta\psi-\pi$. For our case ($\omega_0 Qt_0$ is close to $\frac{3}{2}\pi$ and $\Delta\psi<0$) the curves for the fast and the slow waves are rotated with respect to the vertical axis by the angle $\Delta\psi$ in different directions.

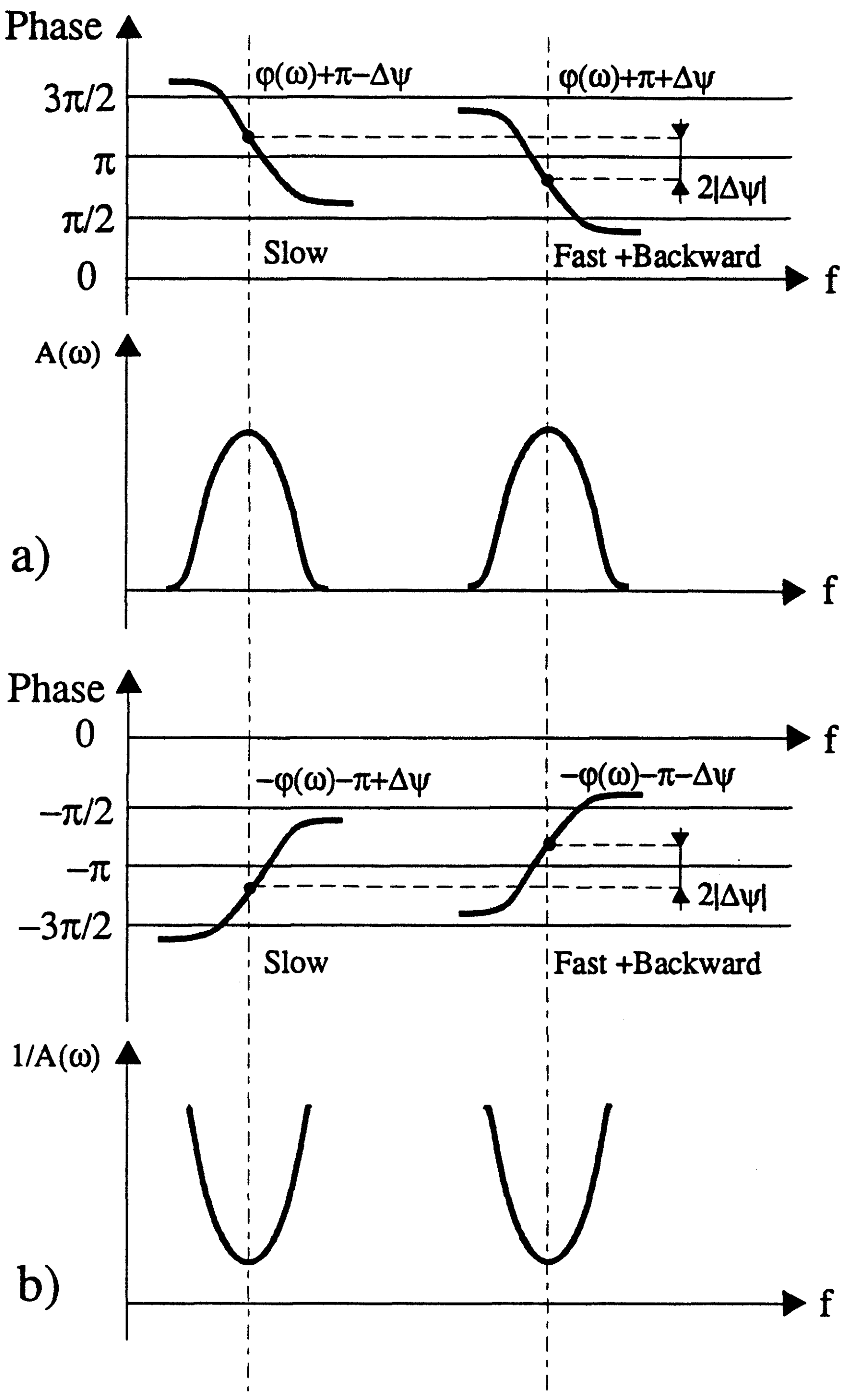

Fig. 9 : Qualitative behavior of the beam response

Usually the theoretical response of the beam is analyzed for the case when the detector and the deflector are installed at the same coordinate $\theta_0 = 0$. In this case the distribution in frequency $G(\Omega)$ of the wave can be obtained, separating the imaginary part of the measured function $1/y$ according to (42). To be able to use this procedure the experimental data must be transformed to the case of the same angular location of the detector and the deflector. Consider how the curves $1/y$ will be transformed for this case. Suppose the deflector is moving to the PU (the relation $t_0 = t_1$ must be kept valid for each position of the deflector). The curves, shown in fig. 10, rotate in the directions, indicated by the arrows: the curves for the fast and the slow waves rotate in the opposite directions. The total angle of rotation when the detector approaches the PU is equal to $\omega_0 Q t_0$. The final position of the curves on the complex plane is shown in fig. 11. The physical meaning of this position of the curves is the following. At resonance (points A and B), the wave of displacement is delayed with respect to the wave of excitation (or the wave of velocity) by $\frac{\pi}{2}$ (fig. 3) for the fast and the backward waves and advances by $\frac{\pi}{2}$ for the slow ones. For the inverse function $1/y$ the phase relations change and the point of the resonance A for the fast and backward waves appears to be rotated with respect to the positive direction of the real axis by the angle $+\frac{\pi}{2}$. Accordingly, for the slow waves the point of the resonance B is rotated by the angle $-\frac{\pi}{2}$.

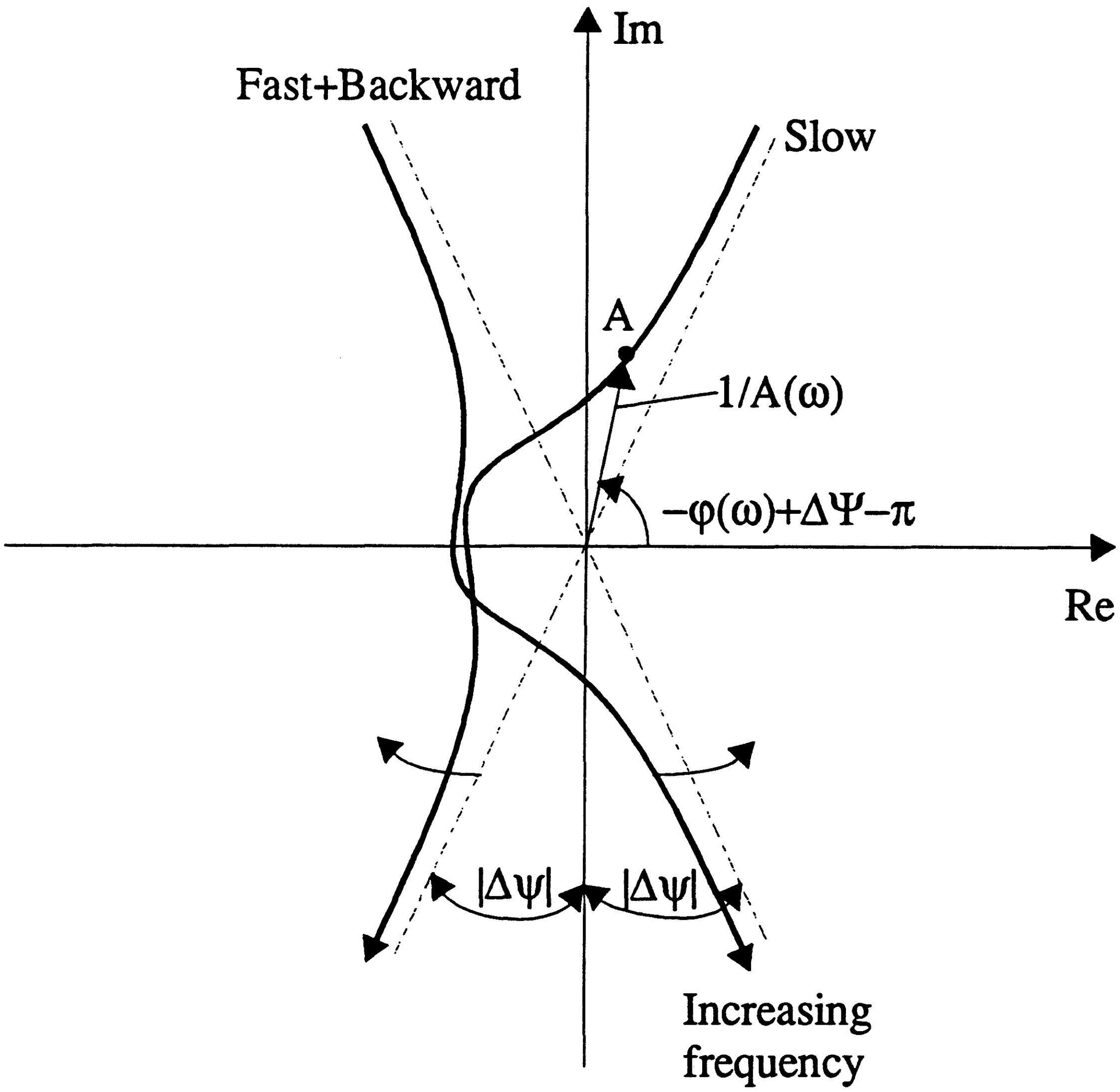

Fig. 10 : Qualitative behavior of the function 1/y in a complex plane.

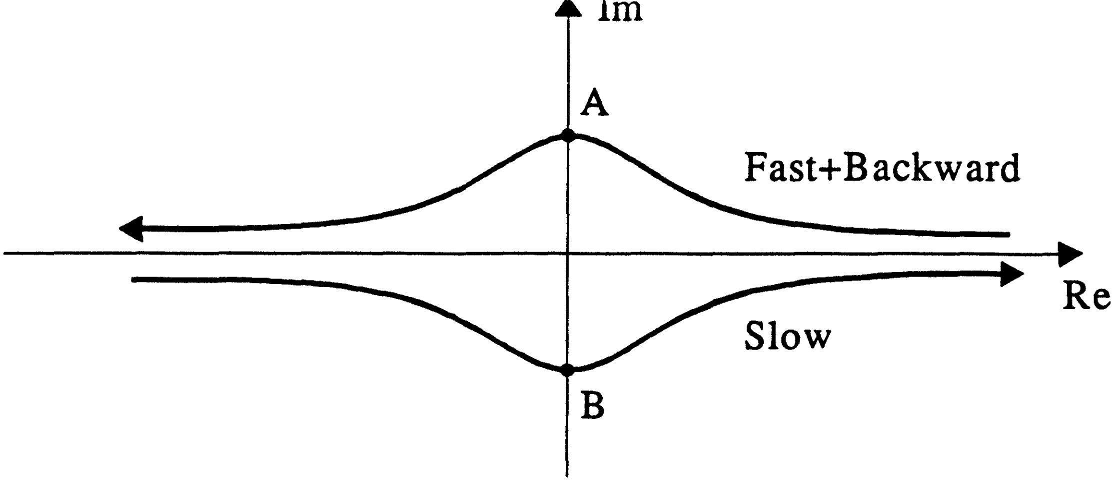

Fig. 11 : Position of curves 1/y in the complex plane when PU and deflector are installed at the same point of the orbit.

Sometimes, when analyzing the coherent oscillations, it is more convenient to consider the response of the wave of velocity y' or the inverse function $1/y'$. The shape of the function $1/y'$ is qualitatively the same as that of $1/y$, but it is rotated by $-\frac{\pi}{2}$ for the fast and backward waves and by $+\frac{\pi}{2}$ for the slow ones. In the case of $\theta_0 = 0$ the functions for the fast, backward and the slow waves qualitatively coincide (fig. 12). When passing through the resonance the phase of the function $1/y'$ changes from $-\frac{\pi}{2}$ to $+\frac{\pi}{2}$. On the contrary for the direct function y' the phase changes from $+\frac{\pi}{2}$ to $-\frac{\pi}{2}$ as for the usual oscillator for all the types of waves.

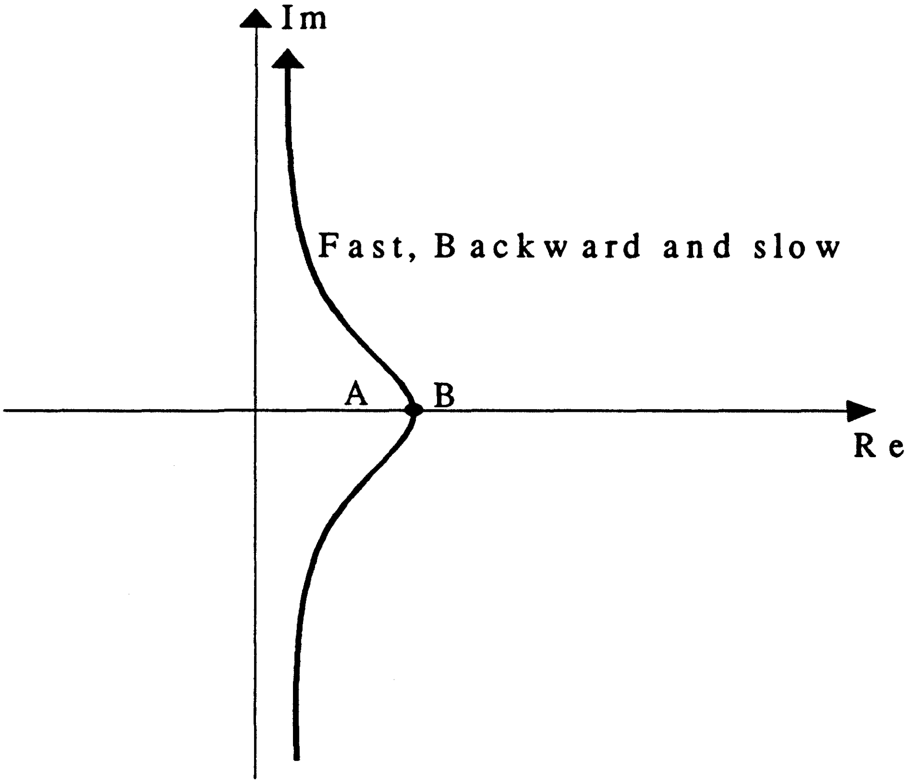

Fig. 12 : Position of curves $1/y'$ (velocity) in the complex plane when PU and deflector are installed at the same point of the orbit.

Now consider the behavior of the function $\varphi_{AB}(\omega)$ outside the resonance. Resonant interaction means that the signals, induced by the particles of the beam in the PU, are summed coherently for multiple turns. When the frequency of excitation is far from resonance the signal is strongly reduced and the main contribution to the summed signal will mainly come from the first turn. When passing through the deflector (fig. 5), the particle is kicked by the electromagnetic field. The signal, induced by this particle in the PU, will be delayed with respect to the field in the deflector by the time $\Delta t = (T - t_0) = \frac{2\pi - \theta_0}{\omega_0}$, where T is the period of revolution. The phase difference of the induced signal and the deflecting field will depend on the frequency as $\omega\Delta t$. Then the phase difference between the points A and B (fig. 5) can be written as:

$$\varphi_{AB} = const - \varphi_1 - \varphi_2 - \frac{2\pi - \theta_0}{\omega_0}\omega \tag{45}$$

where the constant is defined by the phase advance of the betatron oscillations from the deflector to the PU. If $t_0 = t_1$ the latter expression can be transformed to:

$$\varphi_{AB} = const - \frac{2\pi}{\omega_0}\omega \tag{46}$$

One can see that outside resonance the tilt of the function $\varphi_{AB}(\omega)$ will be close to $-\frac{2\pi}{\omega_0}$.

Summarizing, one can imagine the qualitative behavior of the function $\varphi_{AB}(\omega)$, when the frequency is varied over a wide frequency band (fig. 13). Changing the function $\varphi_{AB}(\omega)$ outside the resonance results in changing the "tails" of the function $1/y$ (or $1/y'$) in the complex plain.

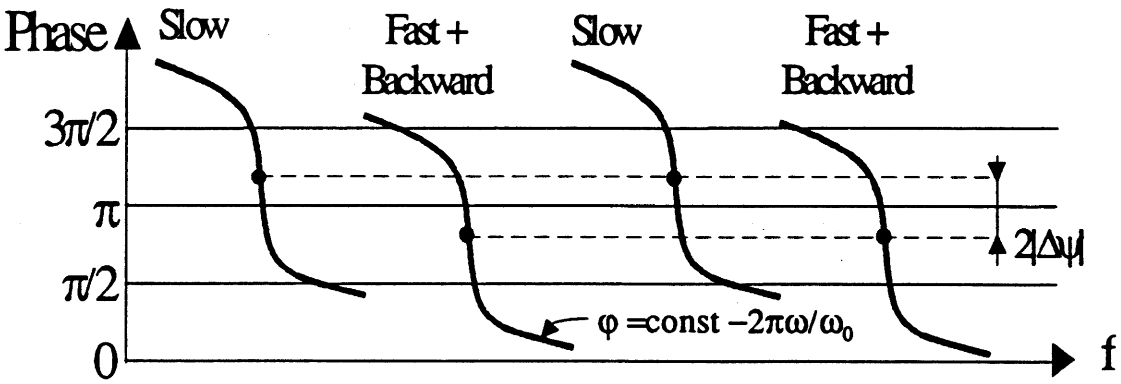

Fig. 13 : Qualitative behavior of the phase response over a wide frequency band.

Fig. 14 shows qualitative behavior of these functions for slow forward and fast (backward) waves at adjacent frequencies. One should note that adjacent-frequency slow and fast (backward) waves correspond to different values of n (fig. 1). For example, near the fifth harmonic of the revolution frequency the wave numbers for the slow and the fast waves are $n_f = 1$ and $n_s = 9$. So, according to (28) the "real" phase difference for these waves will be about $8 \cdot 2\pi$.

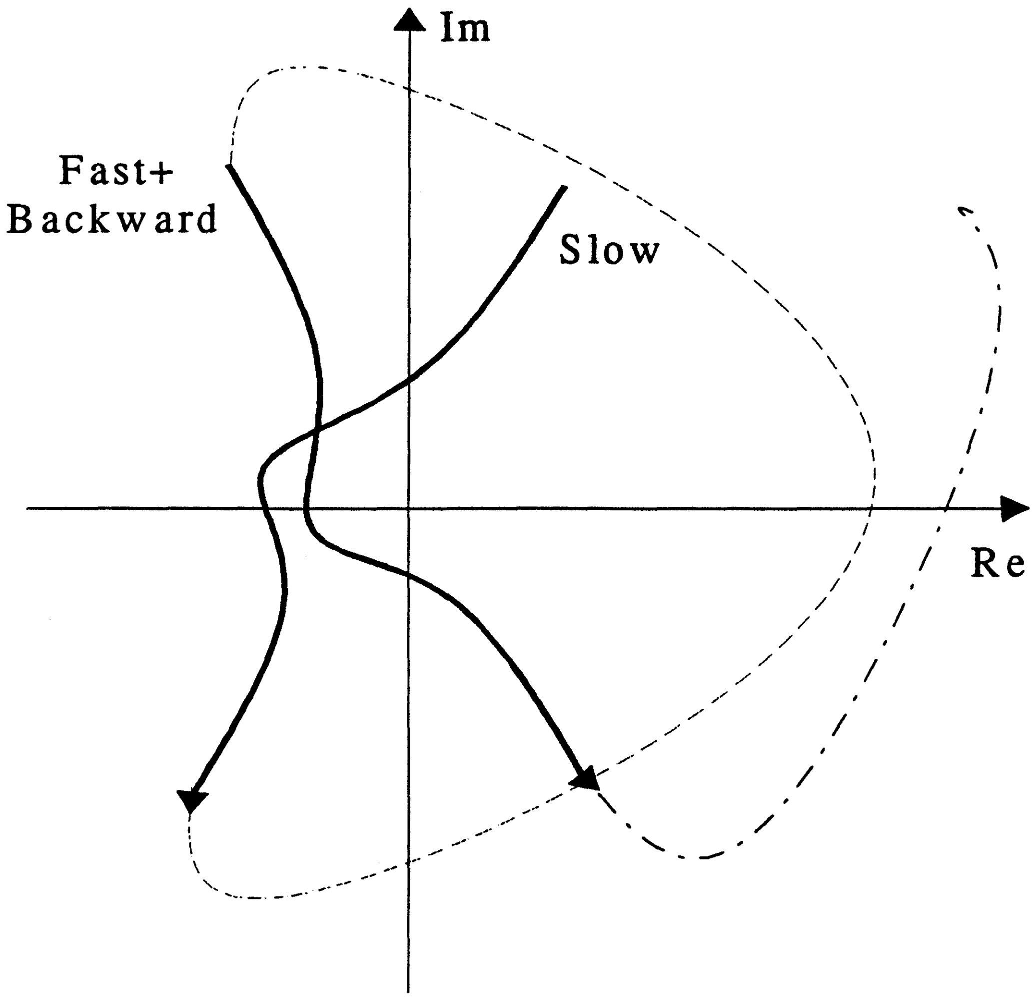

Fig. 14 : Qualitative behavior of 1/y functions in the complex plane for adjacent (in frequency) slow and fast waves.

Up to now we considered the response of the beam with the feedback loop opened and without taking into account interaction of the beam with the fields induced by the beam itself.

Now consider the case, when the fields are still absent but the active feedback loop is closed. In fig. 5 and fig. 6 it is equivalent to turning on the switch "Loop-open/closed". The dimensions of the circuits surrounded by the dashed line are small with respect to the wavelengths of interest. So phase changes inside this region can be neglected. Considering point A as the input and the point B as the output one can draw the block diagram of the system (fig. 15). In this picture I is the transfer function of the system with the opened feedback loop and K is the transfer function of the feedback circuit. Summation of the input and the feedback signals is made at point A.

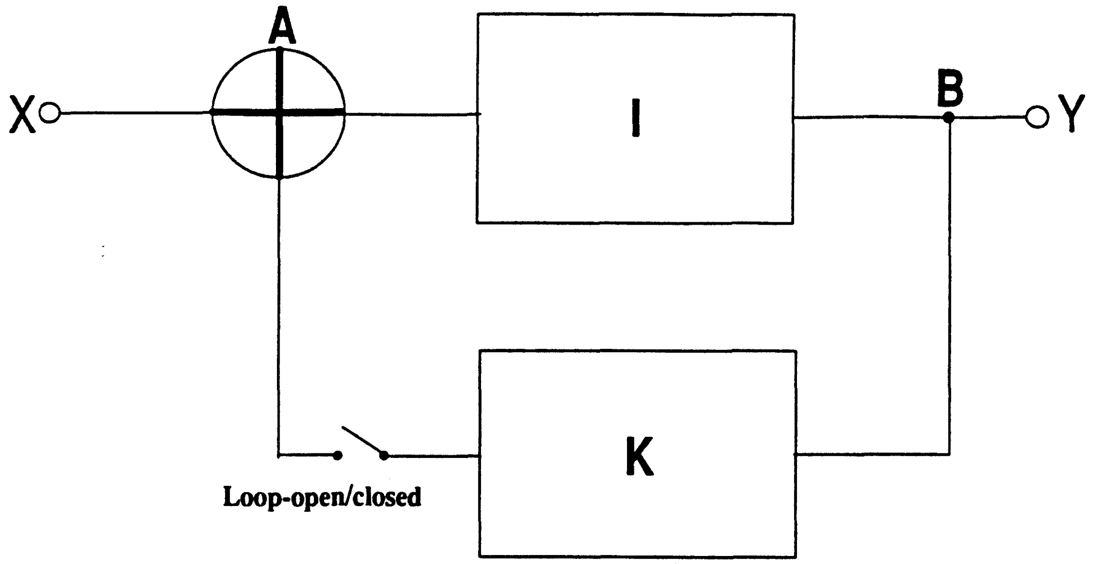

Fig. 15 : Block diagram of the feedback system.

One can write:

$$Y = (KY + X)I \tag{47}$$

and

$$\frac{X}{Y} = \frac{1}{I} - K \tag{48}$$

It can be seen that the function $\frac{X}{Y}$ of the system with the feedback loop closed is the same as that of the system with the opened loop $\frac{1}{I}$, but shifted by the value of the transfer function of the feedback line. In our particular case K is real and it does not depend on frequency. So the experimental functions $1/y$ will be shifted for all the waves by the same value K to the left along the real axis (fig. 16).

The interaction of the beam with the fields, induced by the beam itself on the surroundings is characterized by the impedance (In our case the Transverse impedance). Generally, the impedance is a complex value depending on frequency. The reverse influence of the fields on the beam itself can be considered as existence of an additional feedback. This feedback, similarly to the active one, shifts the function $\frac{X}{Y}$ in the complex plane by some complex value A:

$$\frac{X}{Y} = \frac{1}{I} - K + A \tag{49}$$

Due to dependence of A on frequency, the shift for the different waves will vary.

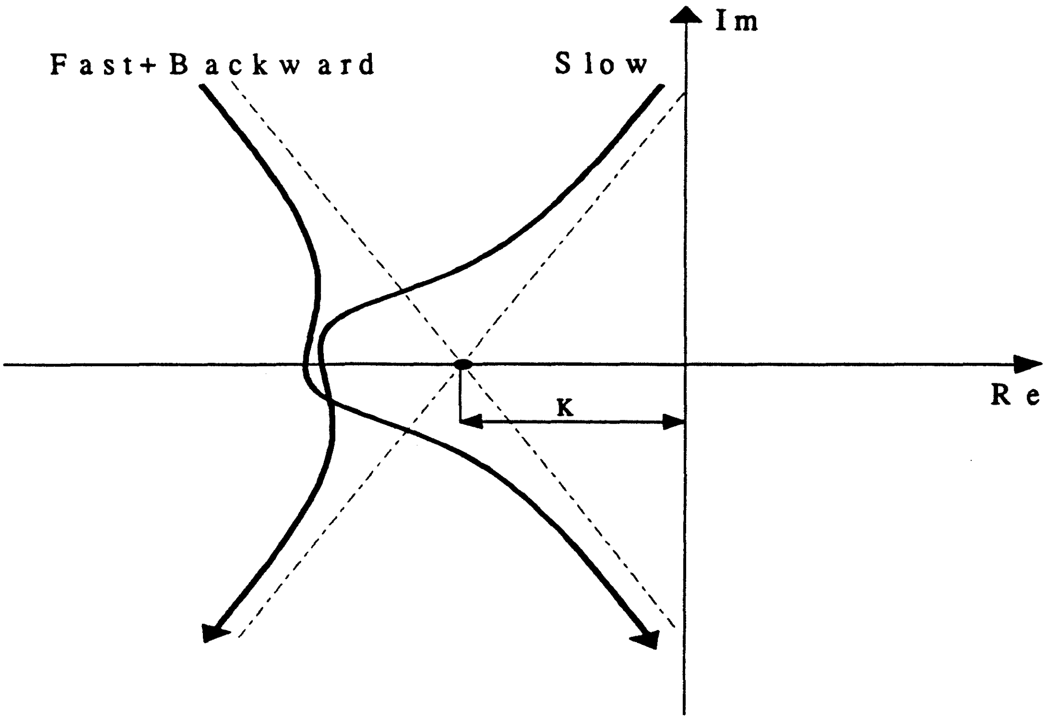

Fig. 16 : Shift of the curves 1/y in a complex plane due to active feedback.

Real measurements of the BTF with the active feedback loop opened are possible only with small intensities of the beam. For typical values of intensities ($10^{11}-10^{12}$ protons/pulse) the measurements are possible only with the closed loop because of beam losses due to instabilities. In this case only the summed effects due to both K and A can be observed. One can separate these effects making measurements for different values of K (of course there must be no losses for all the values of K) and extrapolating the position of the function $1/y$ to the zero value of K. The shift thus found is due to the influence of the fields of the beam and can be used to find the impedance.

Finally one can formulate, how the experimental data of the BTF measurements must be corrected to use them to find the distribution in frequencies and consequently in energies.

1. Outside the resonance the tilt of the phase response resulting in the bending of the tails in the function $1/y$ must be eliminated. (One should note, that this elimination does not influence the final results practically but improves their presentation).

2. Within the resonance curve the correction of the phase distortion in the cables of lengths l_1 and l_2 (fig. 2,6) $\Delta\varphi = \Delta\omega t_1$ must be made.

3. After that the curve $1/y$ must be rotated and shifted in the complex plane to be positioned as it is shown in fig. 11 to satisfy the theoretical relation (42).

4. The imaginary part of the function thus obtained is an unnormalized distribution in frequency $G(\Omega)$. The pulse distribution in the beam can be obtained using (36), (37) or (38) depending on the type of coherent wave of the beam.

4. EXPERIMENTAL STUDY. ANALYSIS OF THE PERTURBATIONS.

The BTF measurements were made in ring 4 of the PS Booster during FLAT cycles using circuits of the damper system for coherent betatron oscillations. The majority of the measurements were made in the horizontal plane for 2 turn injection with an intensity about $8 \cdot 10^{11}$ protons/pulse. Measurements made for 1/2 turn injection as well as in the vertical plane, give qualitatively the same results and are not presented in this report.

The measurements were made with the help of a Hewlett Packard Network Analyzer HP8753C and a Vector Signal Analyzer HP89410A.

The output signal of the Network Analyzer is swept in frequency and its input signal is analyzed after transformation to an intermediate frequency selected by a pass band filter. The band of the separated frequencies depends on a number of parameters but mainly on the band and the time of sweeping as well on the number of digitized points of the signal. The bandwidth of the filter actually fixes the resolution in frequency with which the measurements are being made. Another characteristic of the accuracy of the measurements is time resolution. This parameter is connected with the resolution in frequency, as well as the time and the band of sweeping. Real values of the above mentioned parameters must be taken into account when the measurements are being made and the results are presented and interpreted.

The Vector Signal Analyzer uses frequency analysis of the digitized input signal with the help of an algorithm of the Fast Fourier Transformation (FFT). The output signal can be either a swept frequency sinusoidal signal or white nose in a given frequency band. The frequency resolution Δf of this device depends mainly on the time of measurement T_0. In the simplest (and the best from the point of view of getting higher resolution) case of the uniform window [16] the above parameters are connected by the fundamental relation $\Delta f = 1/T_0$.

Now consider the results of the experiments. Fig. 17 shows the amplitude and the phase responses, measured in the frequency band 0.3-1.5 MHz (0.3 MHz is the lower limit of the operating frequency of the network analyzer HP 8753C). Similar curves have also been measured for other frequencies. The resonant frequencies of the waves agree well with those presented in table 1. As for the response curves, their shapes, particularly the phase characteristics, do not agree with the anticipated ones (fig. 13). The analysis of the possible reasons for the discrepancy enabled conclusions to be made about the influence of the crosstalk in the measuring circuits. Fig. 18 shows amplitude and phase responses measured with the beam off. It can be seen, that the amplitude of the signal is approximately the same as that with the beam outside the resonances (fig. 17). All the efforts to decrease the crosstalk did not succeed, but however it turned out to be possible to separate the signal of interest by vector subtraction of the crosstalk. Amplitude and phase responses thus found are shown in fig. 19. Comparing the amplitude characteristics before (fig. 17) and after subtraction (fig. 19) one can note that the tilt of the curve has disappeared and the ratio of the signals in the resonances and outside has improved by an order of magnitude to become about 10^3. Concerning the phase response, its general behavior is close to that anticipated. When passing through the resonance the phase changes by about -180°. For all the resonances it is close to 180° and is shifted with respect to this level by the small value $\Delta\psi$, the sign of the shift being the same for the fast and the backward waves and different for the slow waves. Outside, but not too far from the resonances, one can distinguish a linear (on average) slope of the curve. Far from the resonances the behavior of the curve becomes irregular due to the reduced useful signal and possible errors in the subtraction of crosstalk.

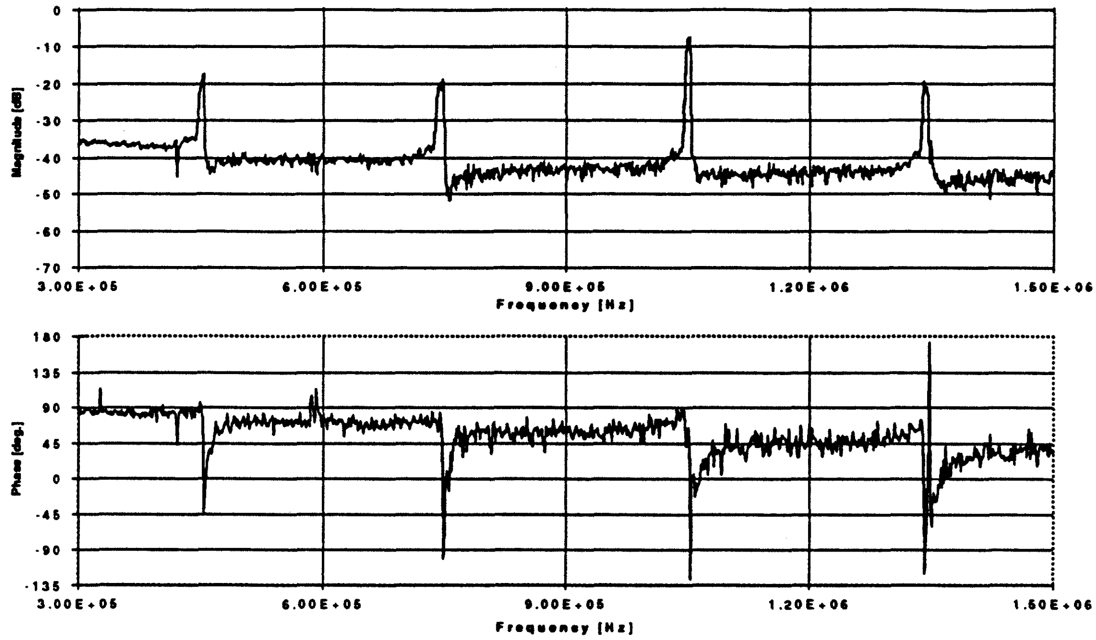

Fig. 17 : Experimental Amplitude and Phase responses (BTF).

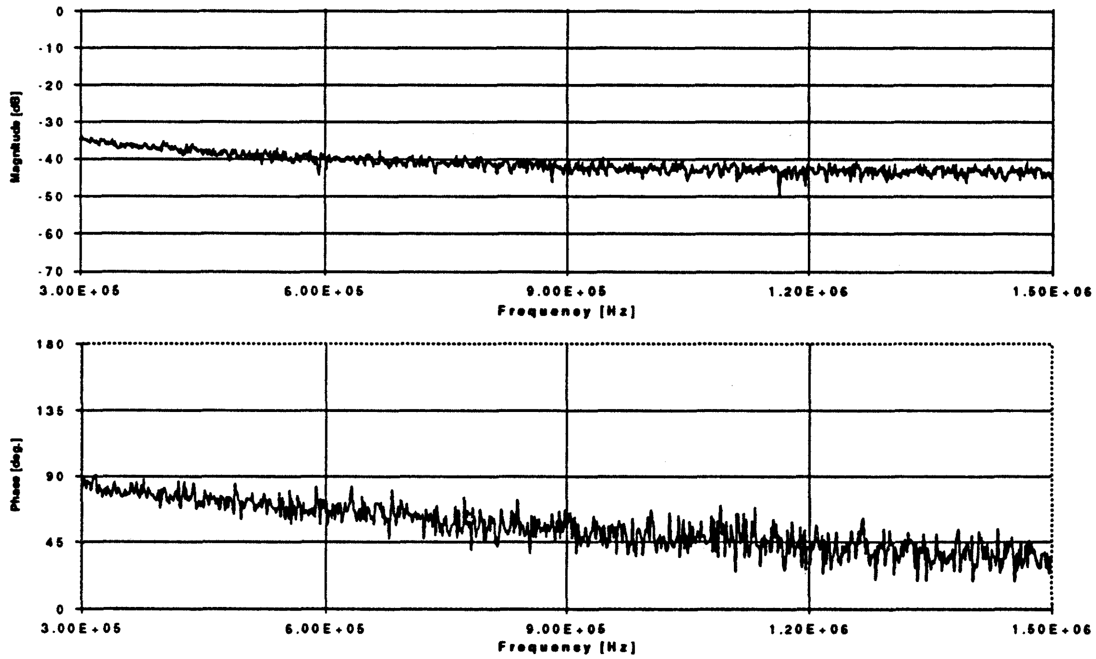

Fig. 18 : Amplitude and Phase responses without beam.

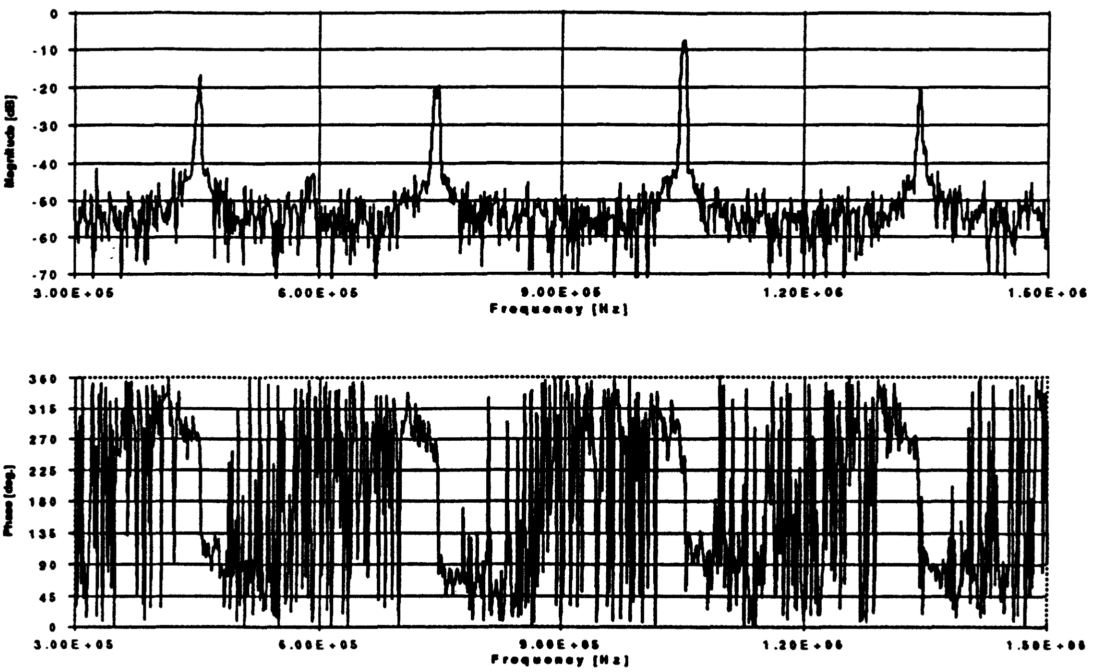

Fig. 19 : Amplitude and phase responses after subtraction of crosstalk.

As mentioned above, the necessary condition for proper operation of a damper of coherent oscillations, is equality of the times of propagation of the beam t_0 and the feedback signal t_1 from the PU to the deflector. Inequality of t_0 and t_1 results in a phase shift (23), which is especially seen at the higher frequencies. Fig. 20 shows amplitude (a) and phase (b) responses, measured for the frequency band 8.7-9.9 MHz, as well as the phase curve (c), measured when a fixed delay equal to $\Delta t = -20$ nsec is removed from the feedback line. One can see the vertical shift $\Delta\varphi$ of the phase response due to the insertion of the delay $\Delta\varphi = -\omega\Delta t$

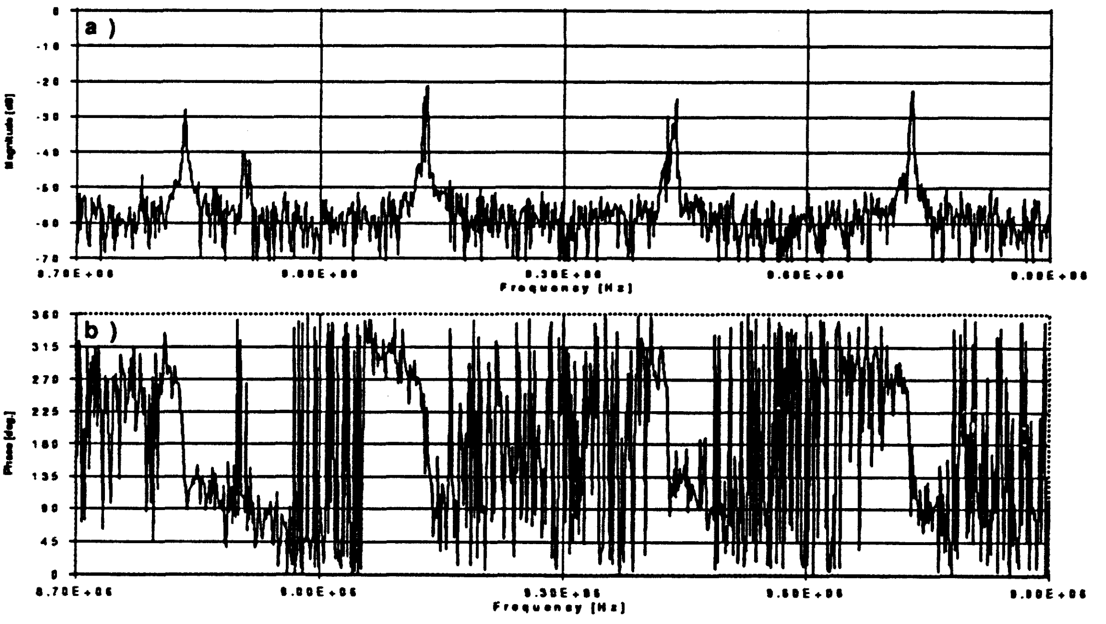

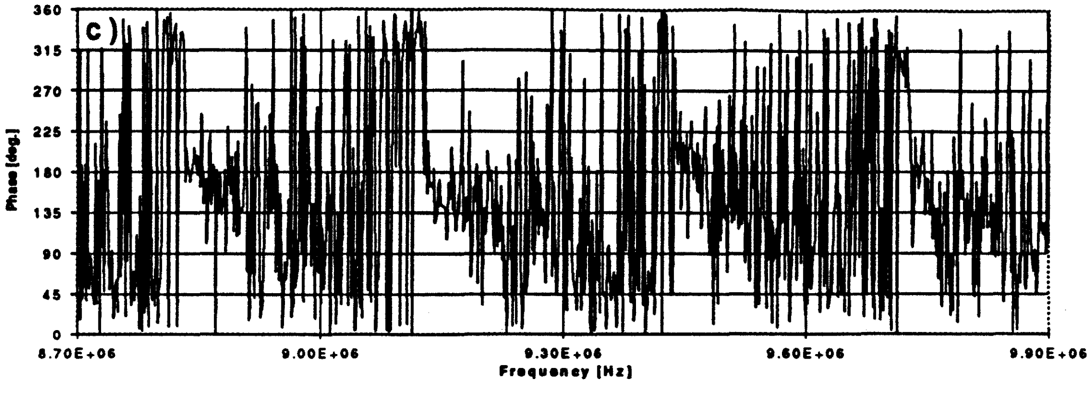

Fig. 20 : Shift of the phase characteristics due to delay error in the feedback line.

Fig. 21 demonstrates the tilt of the phase characteristic outside the resonance. This curve is presented after smoothing for better demonstration. The tilt of the curve is about $-300^{\circ}/600kHz$, which is less than the anticipated value $-360^{\circ}/600kHz$ (47). The difference is evident, because the latter value can be obtained if the signal at the first turn only is detected. This simplification is not valid in general and especially not far from the resonances.

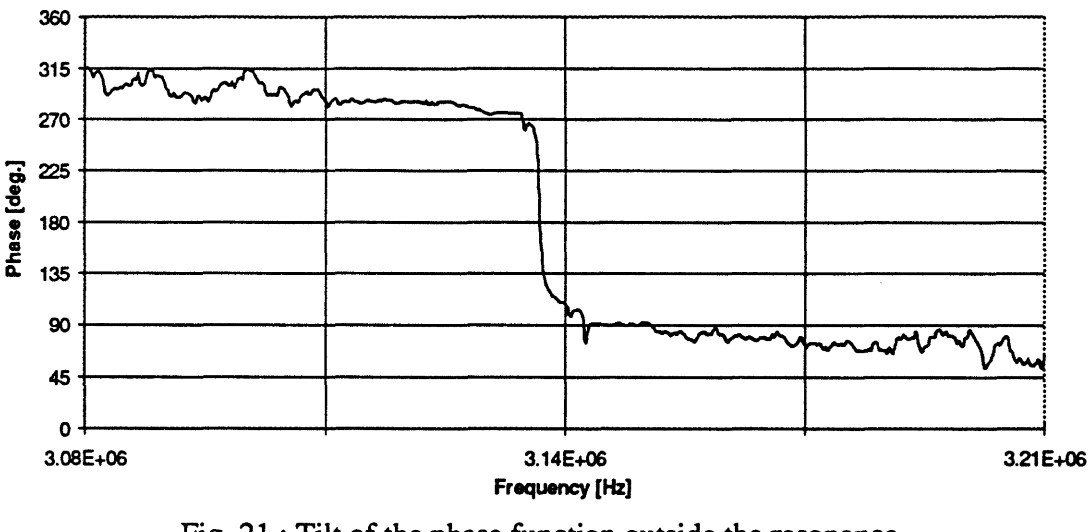

Fig. 21 : Tilt of the phase function outside the resonance.

Now let us begin the analysis of the shapes of the experimental curves. The typical shapes of the curves are shown in fig. 22. Both the phase and the amplitude characteristics are strongly perturbed. The first reason for this perturbation was assumed to be noise of the electronics. To check this assumption the beam was excluded from the line of signal propagation: the signals from the output of the power amplifiers (fig. 5), after proper attenuation, were applied directly to the plates of the PU and observed as with beam. The noise level in this circuit was about 10^3 smaller than the perturbations observed with the beam. The fact that the perturbations decrease outside the resonances also confirms, that they are due to the beam itself.

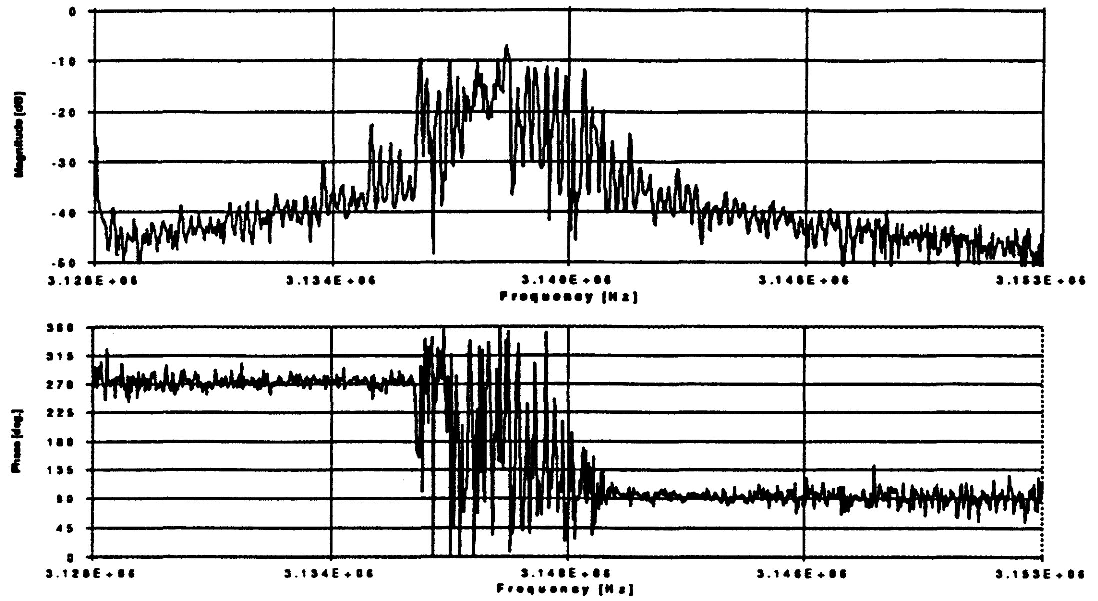

Fig. 22 : Typical response of the Booster beam.

To study the problem of these perturbations measurements of the responses at fixed frequencies (cw) were made. Fig. 23 shows the amplitude response at 3.138 MHz, that is in the middle of the curve given in fig. 22. One can distinguish periodicity of the signal. The Fourier analysis (fig. 24) showed that the signal includes harmonics of 50 Hz. This fact led us to suppose that the modulation of the magnetic fields in the bending and the quadrupole magnets could be a reason for the perturbations. The spectrum of the current of the bending magnets (without the DC component) is shown in fig. 25. This spectrum really includes harmonics of the 50 Hz, but the total ripple of the current is about 10^{-4} (the ripple of the magnetic fields is smaller), which is acceptable from the point of view of normal operation of the Booster. Nevertheless it does not mean that the ripple of the current can not have an undesirable influence on the BTF measurements.

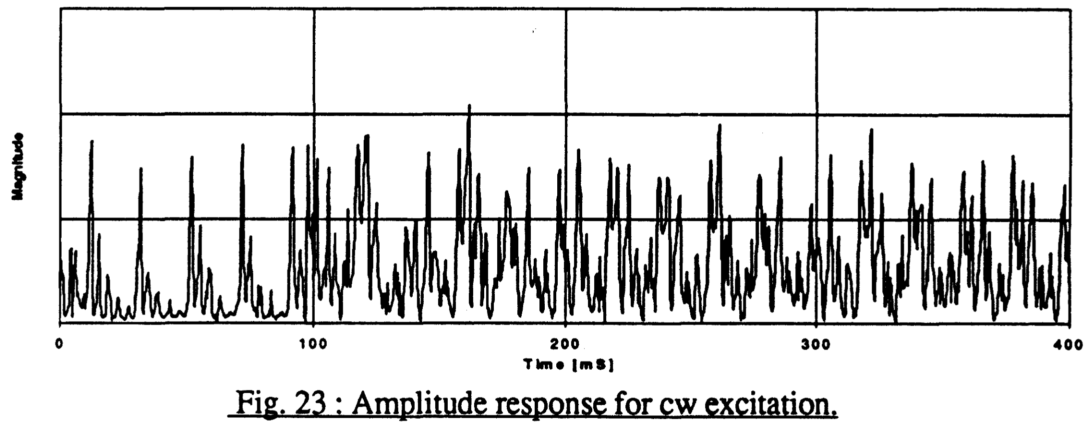

Fig. 23 : Amplitude response for cw excitation.

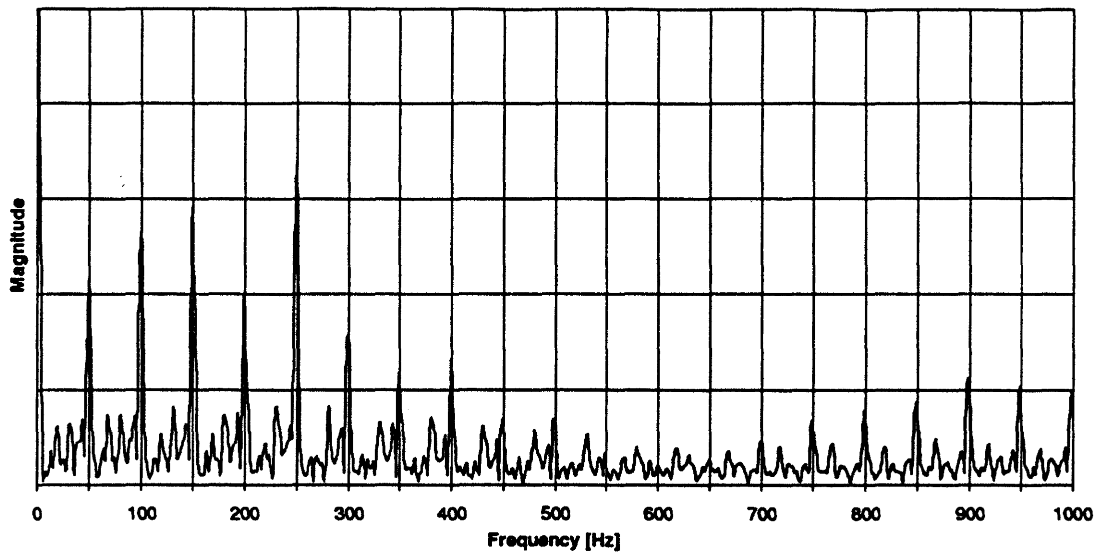

Fig. 24 : Spectrum of the amplitude response for cw excitation.

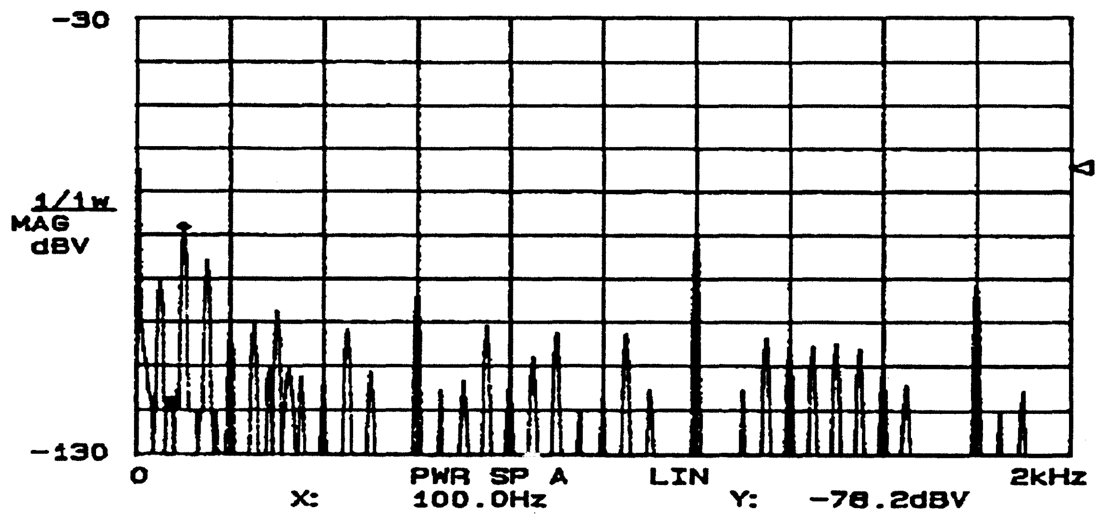

Fig. 25 : Frequency spectrum of the Bending magnet current.

Consider how the ripple of the magnetic fields can influence the modes of coherent oscillations. Suppose that the typical frequencies of the ripple are much smaller than the revolution frequency ω_0. With this assumption the approach described in the first section of this report can still be used but the parameters ω_0, $Q, a_0, b_n, c_n, d_k, e_k\ p_j, q_j, \alpha_0, \beta_n$ and μ_n should be considered as slow functions of time. For small variations of ω_0 and Q one can get the following expressions for the phase velocity $\omega_{ph}(t)$ and the detectable frequency $\omega(t)$:

For fast waves:

$$\omega_{ph}(t) = \omega_0(t)\left[1 + \frac{Q(t)}{n}\right] + \frac{\partial\beta_n(t)}{\partial t}\cdot\frac{1}{n} \tag{50a}$$

For slow and backward waves:

$$\omega_{ph}(t) = \omega_0(t)\left[1 - \frac{Q(t)}{n}\right] + \frac{\partial\mu_n(t)}{\partial t}\cdot\frac{1}{n} \tag{50b}$$

For fast waves:

$$\omega(t) = \omega_0(t)[n + Q(t)] + \frac{\partial\beta_n(t)}{\partial t} \tag{51a}$$

For slow waves:

$$\omega(t) = \omega_0(t)[n - Q(t)] + \frac{\partial\mu_n(t)}{\partial t} \tag{51b}$$

For backward waves:

$$\omega(t) = \omega_0(t)[Q(t) - n] + \frac{\partial\mu_n(t)}{\partial t} \tag{52}$$

One can see that both $\omega_{ph}(t)$ and $\omega\ (t)$ are modulated in time and the system has variable parameters. Even if the wave is excited at a fixed frequency both the phase and the amplitude responses will be modulated in time. Also it should be noted, that the dependence of a_0, b_n and c_n on time in (3) will result in changing of the interaction of the beam's wave and the wave of the exciting force (changing the integral (26)) thus providing an additional amplitude modulation. Moreover, if the time of excitation of the wave is big enough, then parametric resonances are possible.

The effects mentioned above show, that under certain conditions the process under examination can become extremely complicated.

Unfortunately we have no answer to the natural question how big are the modulations (50)-(52) in the PS Booster. But the data available for the machine RHIC [17]($\Delta Q = (45 \div 80)\Delta G/G$, where G is a gradient of the quadrupole fields) indicate that this modulation can be considerable.

In case of a nonzero energy spread in the beam, the modulation of the phase velocities in the linear approximation is the same for all energies. The distribution of phase velocities moves along the velocity axis without changing its shape. Sweeping the frequency of excitation means that the equivalent wave of the deflecting force changes its phase velocity. When the wave of excitation passes the above distribution the energy is transferred to the wave of the beam resulting in the excitation of the coherent oscillations. If the modulation is big enough and fast enough to shift the distribution considerably when the wave of the excitation passes it, the resulting oscillation will not reflect the shape of the distribution and the detectable signals will be distorted.

To confirm this mechanism, a numerical simulation of the response of a set of lossless independent oscillators was made.

Consider a lossless oscillator with a harmonically variable resonant frequency Ω:

$$\Omega = \Omega_0 + A\sin(Rt + \beta) \tag{53}$$

Suppose the oscillation is being excited by the force $f(t) = F_m \sin(\omega t)$ with the frequency ω changing linearly in time $\omega = \omega_0 + kt$. If the variation of ω and Ω are slow then the equation of motion can be written:

$$\frac{d^2 y}{dt^2} + [\Omega_0 + A\sin(Rt + \beta)]y = F_m \sin[(\omega_0 + kt)t] \tag{54}$$

If $A << \Omega_0$, $R << \Omega_0$ and $\omega_0 - \Omega_0 / \omega_0 << 1$ then for the interval of time Δt, such that $k\Delta t << \omega_0$, the variations of ω and Ω can be neglected and the equation (54) can be considered as an equation with non variable parameters:

$$\frac{d^2 y}{dt^2} + \Omega^2 t = F_m \sin(\omega t) \tag{55}$$

The solution of (55) is well known:

$$y = A\sin(\Omega t) + B\cos(\Omega t) + \frac{F_m}{\Omega^2 - \omega^2}\sin(\omega t) \tag{56}$$

The parameters A and B are defined by the initial conditions. Let $y(0) = y_0$, $y'(0) = y'_0$, then

$$y = \left[\frac{y_0'}{\Omega} - \frac{\omega}{\Omega}\frac{F_m}{\Omega^2 - \omega^2}\right]\sin(\Omega t) + y_0\cos(\Omega t) + \frac{F_m}{\Omega^2 - \omega^2}\sin\omega t \tag{57}$$

$$y' = \left[y_0' - \frac{\omega F_m}{\Omega^2 \omega^2}\right]\cos(\omega t) - y_0\Omega\sin(\Omega t) + \frac{\omega F_m}{\Omega^2 - \omega^2}\cos(\omega t) \tag{58}$$

Near the resonance when $\Omega \approx \omega_0$ but $(\Omega - \omega)t << 1$ (57) and (58) can be transformed to

$$y = \frac{y_0'}{\Omega}\sin(\Omega t) + y_0\cos(\Omega t) + \frac{F_m}{2\Omega^2}\sin(\Omega t) - \frac{tF_m}{2\Omega}\cos(\Omega t) \tag{59}$$

$$y' = y_0'\cos(\Omega t) - y_0\Omega\sin(\Omega t) + \frac{F_m}{2}(t - \frac{\Delta\Omega t}{\Omega})\sin(\Omega t) \tag{60}$$

The numerical simulation of the response of the set of oscillators was made in the following sequence:

1. The density distribution function of resonant frequencies was given in n_p points.

2. The initial ω_b and the final ω_e frequencies of the variation of the exciting force as well as the duration of variation T_0 were given.

3. The band of the frequency variation $\omega_e - \omega_b$ and the time T_0 were divided into n_f equal steps inside which the frequency of the force and the resonant frequencies of all the oscillators were considered to be constant.

4. At each step, using (57 and (58 or (59) and (60) the values of y and y' were calculated for n_p points.

5. After each step an average value of $\bar{y}$ for all the n_p points and its maximum value $|\bar{y}|_{max}$ for the period of the exciting force were calculated.

6. For each step the frequency of the exciting force was shifted discretely by the value $k\, T_0 / n_f$ and the resonant frequencies of all the oscillators were changed according to (53). The values of y and y' calculated at the previous step were taken as the initial conditions. For the first step it was supposed $y_0 = y'_0 = 0$, that is the system was initially considered at rest.

7. As a result of the simulation, the dependencies of $|\bar{y}|_{max}$ on frequency or on time were obtained.

The initial distribution of the resonant frequencies was supposed to be Gaussian with the central frequency 3000 kHz, dispersion $\sigma = 1$ kHz and was given for n_p=10000 points within the interval $\pm 3\sigma$.

Fig. 26 shows the function $|\bar{y}|_{max}(t)$, calculated for the following parameters: $\omega_e = \omega_b = 2\pi \cdot 3000$ kHz, $R = 2\pi \cdot 50$ Hz, $A = 2\pi \cdot 1$ kHz, T_0=400 msec, n_f=1000. The shape of the curve is rather complicated, but as for the experimental curve (fig. 23) one can distinguish its periodicity. The frequency spectrum of the simulated curve is given in fig. 27. One can see that a simple sinusoidal modulation of resonant frequencies of the oscillators results in a rather complicated spectrum of the resulting function $|\bar{y}|_{max}(t)$.

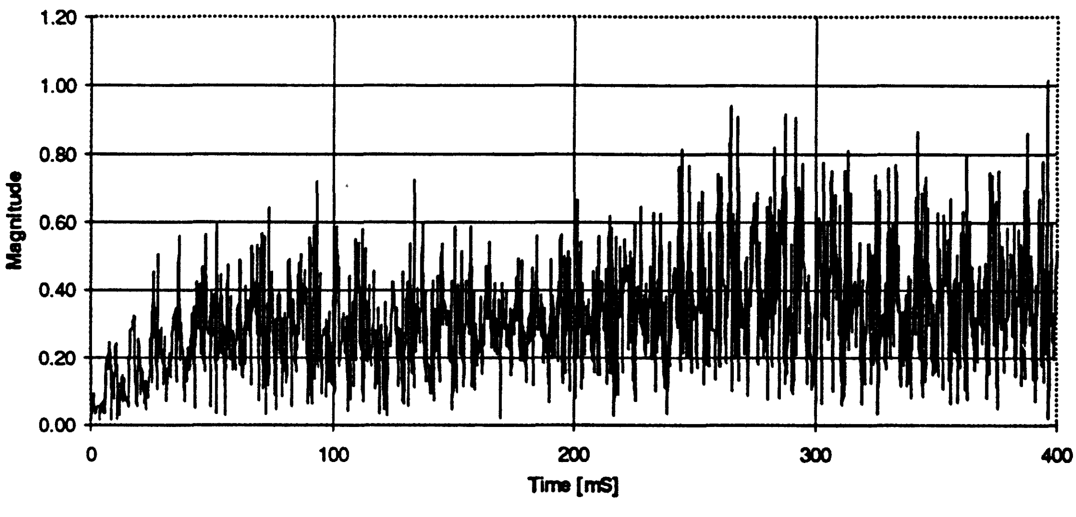

Fig. 26 Simulated curve of the amplitude response for fixed frequency (cw).

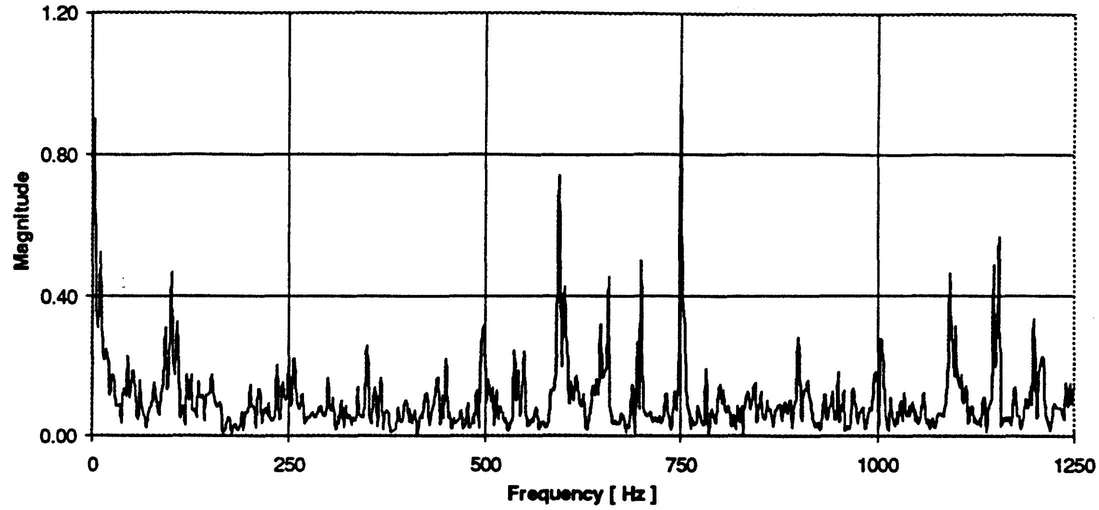

Fig. 27 : Frequency spectrum of the simulated (fig. 26) amplitude response.

The degree of perturbation depends on the duration of sweeping. Fig. 28(a,b) shows two curves of $\left|y\right|_{max}(t)$, calculated for the same values of $\omega_b = 2\pi \cdot 2995$ kHz, $\omega_e = 2\pi \cdot 3005$ kHz, $\beta = 0$, $R = 2\pi \cdot 50$ Hz, $A = 2\pi \cdot 1$ kHz and $n_f = 1000$ but for different duration: $T_0 = 4$ msec and $T_0 = 400$ msec. The shape of the function $\left|y\right|_{max}(t)$ also depends on the phase β of the modulation. Fig. 28c shows the function $\left|y\right|_{max}(t)$, calculated for the duration $T_0 = 4$ msec and $\beta = \pi$.

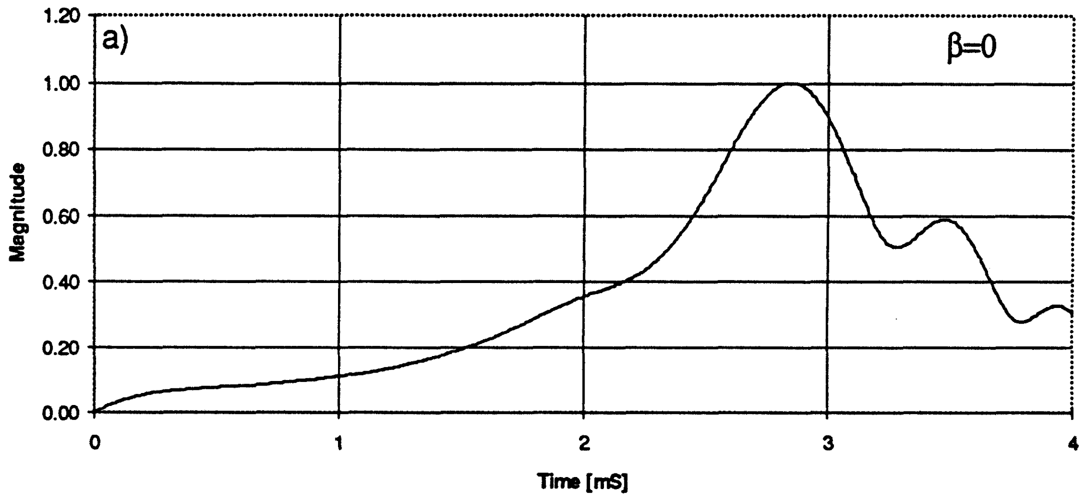

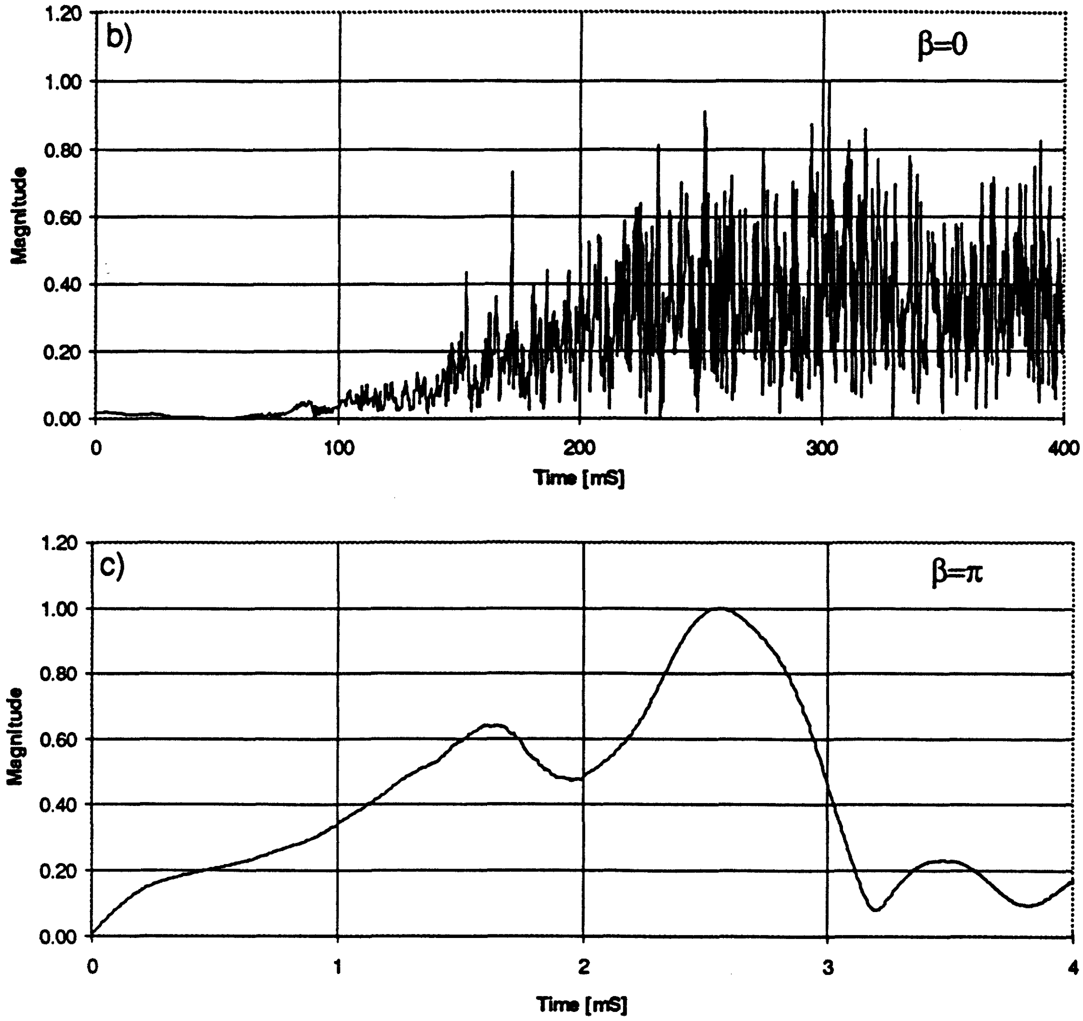

Fig. 28 : Amplitude responses for different durations of sweeping time and different phases of the modulation function.

One should note, that the numerical model used is rather rough to be applied for a quantitative description of the experimental effects. It does not take into account the effect of finite resolution in frequency of the measuring device, damping of the coherent oscillations and some other effects.

To decrease the perturbations one should decrease the time of measurement. However one should understand that the decrease is limited by the following:

1. The time of measurements must be much bigger than the period of the beam revolution (1.67 μsec in our case) to provide a resonant excitation.

2. When the duration of the measurements decreases the resolution in frequency is degraded. According to (36)-(38) and the list of Booster parameters [15], the frequency width of the resonances must be several kHz. To measure the shape of the distribution the resolution in frequency must be at least 10 times smaller, for example 250 Hz. To provide this resolution the time of observation of the signal must be at least 4 msec. The results of numerical simulations have shown that for T_0=4 msec there are important perturbations even for the simplest sinusoidal modulation with the 50 Hz frequency. According to the spectrum of the current in the bending magnets (fig. 25), one can suppose that the function of modulation of the resonant frequencies of the coherent modes is more complicated and rapid. The "fast"

measurements made with the help of the Vector Signal Analyzer confirmed the above considerations. Fig. 29 shows the amplitude responses measured for different values of T_0. As anticipated the perturbations increase with the increasing of T_0. However one should note that the observed perturbations increase, not only because of the increase of time, but also due to a simultaneous improvement of frequency resolution. Fig. 30 shows the behavior of the amplitude response for different moments in time within one beam pulse. Strong variation of the response for this particular measurement can be explained by the variations of the magnetic fields.

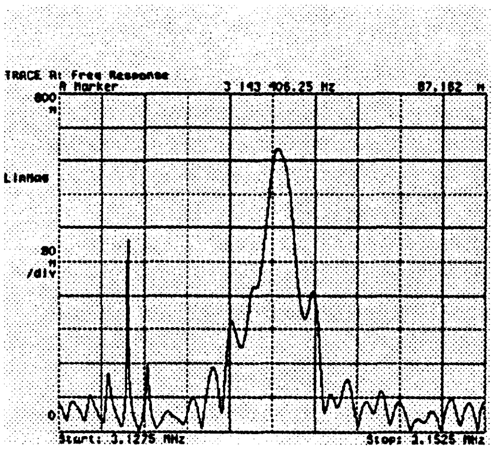

$T_0 = 1mS$

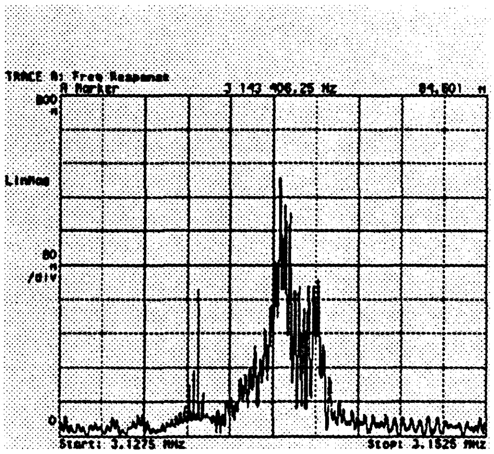

$T_0 = 4mS$

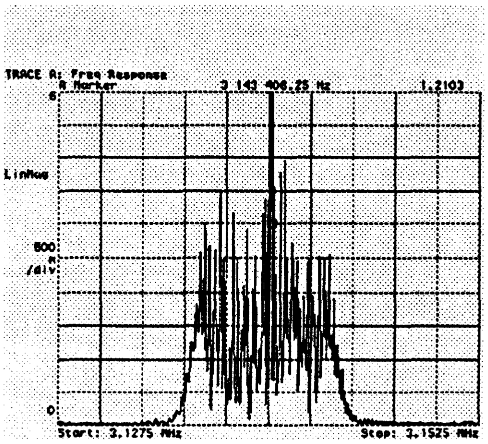

$T_0 = 16mS$

Fig. 29 : Amplitude responses for different values of measurement duration.

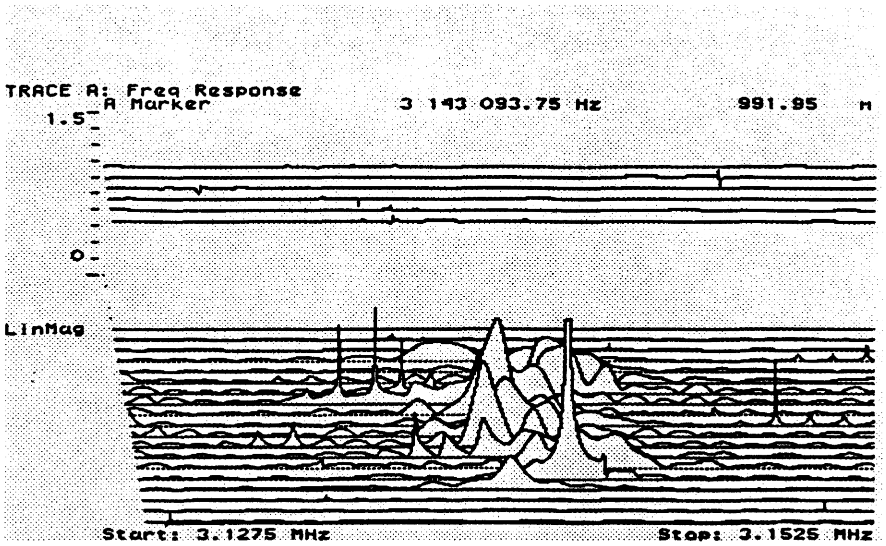

Fig .30 : Waterfall display. Successive amplitude responses within one beam pulse.

Summarizing the above considerations it is possible to conclude that when making BTF measurements we are dealing with a typical unsteady process. The time which is required to observe the process is larger than the characteristic time for it to change.

The direct way to avoid the fluctuations is to improve the stability of the magnetic fields but this in practice is not a trivial affair. Another way is using a technique of restoration of experimental functions [18].

The results of measurements of any characteristic are always distorted by the measuring device and the function measured always differs from a real one.

Let $\Phi(\xi)$ be a real function and $F(x)$ a measured one. A constraint of these two functions is described by the integral Fredholm equation of the first kind:

$$F(x) = \int_{\xi} K(x,\xi)\Phi(\xi)d\xi \qquad (61)$$

The kernel of the equation $K(x,\xi)$ is a characteristic of the device. For a fixed value of $\xi = \xi_0$ the function $K(x,\xi_0)$ is a response of the device to a δ-function signal $\delta(\xi - \xi_0)$. If the characteristics of the device are known, that is the function $K(x,\xi)$ is known, then the equation can be solved and the real function $\Phi(\xi)$ can be found in spite of the perturbations by the device. The function $K(x,\xi)$ can hardly ever be found experimentally. But sometimes it can be calculated with an acceptable accuracy.

In the case of the BTF measurements the whole system, including the signal analyzer, measuring circuits and the accelerator, should be considered as a single measuring device from the point of view of perturbation of the real distribution in frequencies. The equations of the type of (61) can be formulated for the amplitude and the phase response functions independently.

The most complicated step in finding the kernels $K(x,\xi)$ for the amplitude and the phase functions is taking into account a law of modulation. The modulation is due to distortion of magnetic fields, but as all the considerations are being made within the model of a set of harmonic oscillators it is sufficient to know a law of modulation of frequencies or phase velocities of eigen modes. According to (5), (6) and (6a) the modulation of the revolution frequency ω_0 and tune Q can be considered as the origin of modulation of the eigen frequencies and phase velocities . The measurements done showed that there is no reproducibility of BTF measurements; neither within the beam pulse (fig. 30) nor from one pulse to another. In this case the modulations of ω_0 and Q must be measured simultaneously with the BTF. It can be done by measuring a response of the system to the excitations at different frequencies simultaneously, as shown in fig. 31. The measurements can be made with the help of two Vector Signal Analyzers triggered simultaneously. The BTF measurements are made by the analyzer FFT1. The second analyzer FFT2 operates at the fixed frequency ω_2 far from any resonance. To understand the behavior of the system at the frequency ω_2 one can apply a simplified model of single turn interaction (no resonance), used previously in section 3. Fig. 32 shows a behavior of the beam when passing through the deflector and the PU. Let the field in the deflector be described by the function $\sin(\omega_2 t)$. When the beam passes through the deflector its transverse momentum is modulated by this function and the coherent transverse oscillations are excited. Phase advance of the coherent oscillations from the deflector to the PU can be written as $Q(2\pi - \theta_0)$. Taking into account the time of flight from the deflector to the PU $(2\pi - \theta_0)/\omega_0$, the displacement of the beam in the PU and hence the induced signal can be written as

$$U(t) = \sin[\omega_2(t - \frac{2\pi - \theta_0}{\omega_0})] \cdot \sin[Q(2\pi - \theta_0)] \qquad (62)$$

If ω_0 and Q vary in time then the signal (62) appears to be modulated both in phase and in amplitude, in the case of a single turn interaction the amplitude modulation being due to tune variation and the phase - due to revolution frequency modulation.

The model of a single turn interaction is presented for the explanation only. Really, when calculating the modulations of ω_0 and Q not only the first but also a number of subsequent turns must be taken into account.

After the function of modulation of the eigen frequency has been found one has to calculate the displacement of the monochromatic beam in the PU at a frequency close to the resonance for the law of excitation provided by the FFT1 for the time interval T_0 equal to the time of measurement of this device. Then the function of displacement must be Fourier transformed using the same algorithm as in the FFT1.

As a result the response of the whole system, now considered as a "device", can be found for a monochromatic beam as a function of frequency. That is the kernel of the equation (61) for a fixed ξ_0 can be found. Due to linearity of the system within the frequency band of interest, near the resonance, the kernels for other values of ξ are the same as that for the ξ_0 but shifted along the frequency axis by the appropriate value.

After the kernel $K(x,\xi)$ has been found one can solve the equation (61) and find a real function of distribution in frequency or in momentum.

Above are presented only general considerations on the application of the method of restoration of experimental functions for the BTF measurements. A conclusion about the possibility of applying this technique cannot be made without further experimental and theoretical studies.

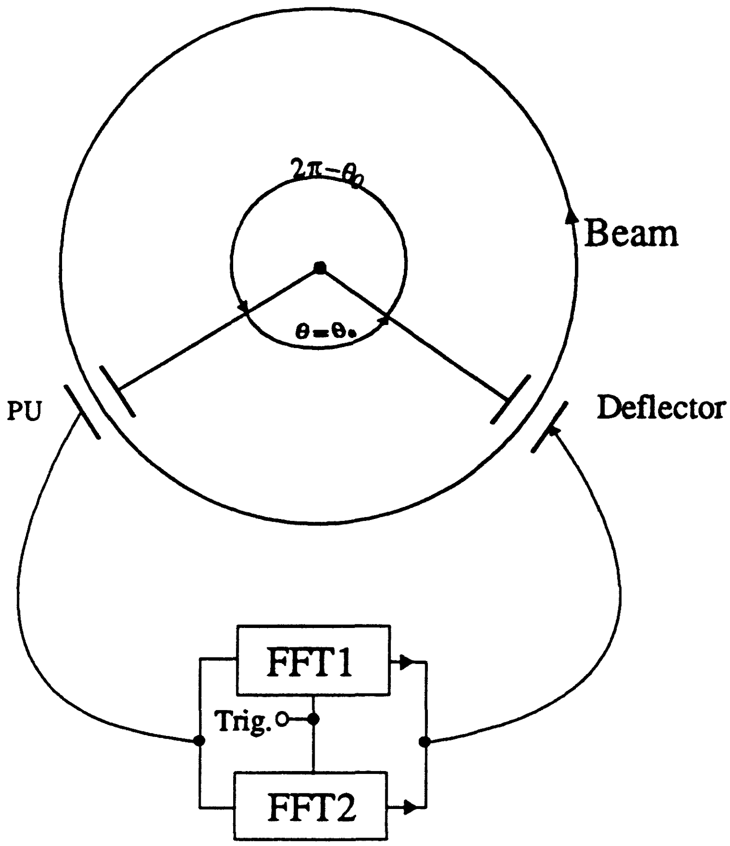

Fig. 31: Simultaneous measurements of beam responses at two frequencies.

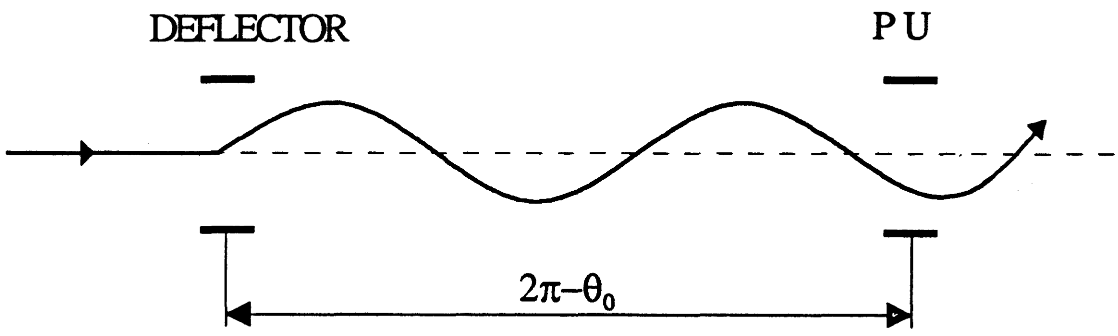

Fig. 32: Behavior of the beam in a single turn model.

CONCLUSION

Attempts at BTF measurements of the coasting beam in the CERN PS Booster are described in the report. The peculiarity of the measurements is the use of the circuits of the active feedback loop on special cycles during normal operation of the machine. This feature resulted in necessity of the combined qualitative consideration of the coherent processes in the beam and operation of the active feedback system. A Qualitative analysis of the effects which can be observed experimentally is also presented. Real experimental results in general agree with those predicted but appear to be strongly perturbed. The analysis of the signals enabled an assumption to be made about the influence of the fluctuations of currents in the bending and the quadrupole magnets. These fluctuations result in modulation of phase velocities of the eigen modes of coherent oscillations. Further spectral analysis of the fluctuations of currents in the bending magnets, as well as a simplified numerical simulation of the process, confirmed the assumption. The fluctuations of magnetic fields of about 10^{-4} though negligible from the point of view of normal operation of the accelerator, appear to be disastrous for the BTF measurements. When measuring a BTF we are dealing with an unsteady process, the typical time of measurement being larger than the typical time of variation of the characteristics of the eigen modes. To decrease the time for a measurement requires an unacceptable degradation of the resolution in frequency.

The way out of the situation can be to use the method of restoration of dependencies through the perturbed experimental results. The most complicated problem of taking into account the law of fluctuations of the magnetic fields can be eliminated by making beam response measurements at two frequencies simultaneously. But a conclusion about the possibility of applying the technique cannot be made without further research and detailed simulation of the processes.

ACKNOWLEDGMENTS

The authors would like to thank F. Caspers, V.Moiseev, F.Pedersen, K.Schindl H.O.Schonauer and D. J. Williams for discussions, help and consultations.